TLR8 senses *Staphylococcus aureus* RNA in human primary monocytes and macrophages and induces IFNβ production via a TAK1-IKKβ-IRF5 signaling pathway

Bjarte Bergstrøm, Marie H. Aune,* Jane A. Awuh,* June F. Kojen,* Kjetil J. Blix,* Liv Ryan,* Trude H. Flo,* Tom E. Mollnes,*[,†,#,‡,§] Terje Espevik,*[,1] and Jørgen Stenvik*[,1]*

*Centre of Molecular Inflammation Research, Department of Cancer Research and Molecular Medicine, Norwegian University of Science and Technology, Trondheim, N-7491 Norway

[†]Department of Immunology, Oslo University Hospital Rikshospitalet, Oslo N-0027, Norway

[#]K.G. Jebsen Inflammation Research Center, University of Oslo, Oslo N-0027, Norway

[‡]Research Laboratory, Nordland Hospital, Bodø N-8092, Norway

[§]Institute of Clinical Medicine, University of Tromsø, Tromsø N-9037, Norway

[1]T.E. and J.S. are co-senior authors

Running Title: *S. aureus* activates a TLR8-TAK1-IKKβ-IRF5 axis in monocytes

Correspondence: Jørgen Stenvik, jorgen.stenvik@ntnu.no, Phone: +47 72825343, Fax: +47 72571463

This work was supported by the Liaison Committee between the Central Norway Regional Health Authority (RHA) and the Norwegian University of Science and Technology (NTNU) (project numbers 46056622 and 46056633) and by the Research Council of Norway through its Centres of Excellence funding scheme, project number 223255/F50.

Abstract

Staphylococcus aureus may cause serious infections and is one of the most lethal and common causes of sepsis. TLR2 has been described as the main pattern recognition receptor (PRR) which senses SA and elicits production of pro-inflammatory cytokines via MyD88-NF-κB signaling. SA can also induce the production of IFNβ, a cytokine that requires interferon regulatory factors (IRFs) for its transcription, but the signaling mechanism for IFNβ induction by SA are unclear. Surprisingly, we demonstrate that activation of TLR2 by lipoproteins does not contribute to IFNβ production but instead can suppress the induction of IFNβ in human primary monocytes and monocyte-derived macrophages (MDMs). The production of IFNβ was induced by TLR8-mediated sensing of SA RNA which triggered IRF5 nuclear accumulation, and this could be antagonized by concomitant TLR2 signaling. The TLR8-mediated activation of IRF5 was dependent on TAK1 and IKKβ, which thus reveals a physiological role of the recently described IRF5-activating function of IKKβ. TLR8-IRF5 signaling was necessary for induction of IFNβ and IL12 by SA, and it also contributed to the induction of TNF. In conclusion, our study demonstrates a physiological role of TLR8 in the sensing of entire SA in human primary phagocytes, including the induction of IFNβ and IL12 production via a TAK1-IKKβ-IRF5 pathway that can be inhibited by TLR2 signaling.

Abbreviations

HK, heat-killed; HS, human serum; IKK, IkB kinase; IRF, interferon regulatory factor; L2K, Lipofectamine 2000; *lgt*, prolipoprotein diacylglyceryl transferase gene; NOD2, nucleotide-binding oligomerization domain-containing protein 2; PAMP, pathogen associated molecular pattern; PRR, pattern-recognition receptor; pI:C, polyriboinosinic polyribocytidylic acid; pL-arg, poly-L-arginine; pU, polyuridylic acid; RIP2, receptor interacting protein 2; SA,

Staphylococcus aureus; STING, stimulator of interferon genes; TAK1, transforming growth factor β-activated kinase 1; TBK1, TANK-binding kinase 1; wt, wild-type.

Introduction

Staphylococcus aureus (SA) can act as a peaceful colonizer of the skin and the nostrils or as an aggressive pathogen causing invasive diseases and sepsis. Intracellular survival of SA, abscess formation, as well as the emergence of methicillin resistant strains complicate the treatment of serious infections (1). SA also produces virulence factors such as hemolytic and leucolytic toxins and C-targeting factors which contribute to immune evasion (2). TLR2 is a primary PRR for sensing of SA by immune cells and mediates resistance of mice against experimental SA infection (3). SA deficient in lipoprotein synthesis (*Δlgt*) does not activate TLR2 and elicit reduced pro-inflammatory responses in human cell lines (4). Children and teenagers with MyD88- or IL1R-associated kinase 4-deficiency are at risk of infections with pyogenic bacteria, in particular SA, *Streptococcus pneumonia*, and *Pseudomonas aeruginosa* , while their resistance against infection with other pathogens is normal (5, 6). This indicates a particular importance of TLR2 and/or IL1Rs for resistance against SA infection in young humans.

Type I IFNs are classical antiviral cytokines, but they are also induced by intracellular and extracellular bacteria. The impact of the main Type I IFNs (IFNα and IFNβ) on bacterial infections is less clear and spans from enhanced innate and cell-mediated immunity to immune suppression and dysregulation which may contribute to the progression of septic shock (7). The predominant pathway of IFNβ induction by Gram negative bacteria is by LPS-mediated activation of endosomal TLR4 signaling via the TIR-domain containing adapter inducing IFNβ-IRF3 pathway (8, 9). For Gram-positive bacteria there may not be a single predominant mechanism for IFNβ induction as multiple pathogen-associated molecular patterns (PAMPS) and cell host receptors have been implicated in different model systems. In murine phagocytes recognition of bacterial RNA and DNA appears as central for IFNβ production (10–12), and mouse TLR13 was recently identified as a sensor of RNA of

microbial origin (13, 14). Induction of type I IFNs by SA has been examined in different human and murine cell types with different conclusions regarding the molecular mechanisms involved. SA PAMPs suggested to be responsible for IFNβ induction include staphylococcal protein A (SpA), DNA, RNA, and lipoteichoic acid, and TLR2, TLR7, TLR9, and cytosolic PRRs were implicated (15–22).

The aim of the present study was to examine the role of TLR2 and other PRRs for SA-induced IFNβ production in human primary monocytes and MDMs. Unexpectedly we found that TLR2 activation could suppress the SA-induced production of IFNβ. In contrast, induction of IFNβ was triggered by SA RNA which activated a TLR8-IRF5 signaling axis in a TAK1 and IKKβ dependent fashion. We here establish TLR8 as a second MyD88 dependent PRR of SA in human primary monocytes and MDMs and show that it is essential for the induction of IFNβ production by whole bacteria via a recently identified IKKβ-IRF5 activation pathway. We also demonstrate a cross-regulatory function of TLR2 in TLR8-IRF5 signaling.

Materials and Methods

Materials

Concentrations of IFNβ were determined with the VeriKine-HS^{TM} Human Human Interferon-Beta Serum ELISA Kit (PBL Assay Science, Piscataway, NJ) typically with no dilution or 1:2 dilutions of the culture supernatants. BioPlex assays were from BioRad and were analyzed as per the manufacturer with dilutions of the supernatants ranging from none to 200, depending on the cytokine to be examined. *E. coli* bioparticles was of the rough K12-strain (Invitrogen). The following TLR-ligands were from Invivogen: LPS from the *E. coli* K12-strain, FSL-1, Pam3Cys, R837, CL75, polyriboinosinic polyribocytidylic acid (pI:C), and polyuridylic acid (pU). Lipofectamine 2000 (L2K) was from Invitrogen, while poly-L-arginine (pL-Arg) was from Sigma-Aldrich. RNAse A was from Qiagen. The IKKβ-inhibitor BI605906 was generously provided by prof. Sir Philip Cohen (University of Dundee, Scotland), while IKKII-VIII and the TAK1 inhibitor 5z-7-oxozeanol was from Calbiochem/MerckMillipore (Darmstadt, Germany). The TAK1 inhibitor NG-25 was from MedChem Express (Monmouth Junction, NJ).

Bacteria and bacterial lysates

Staphylococcus aureus 113-wild type strain, its isogenic 113*Δlgt* mutant, and the pRBlgt-reconstituted 113*Δlgt* strain were generously provided by prof. Friedrich Göetz (University of Tübingen, Germany). The Newman and Cowan strains were generously provided by prof. Timothy Foster (Trinity College, Ireland), while the Wood-46 strain was from ATCC (10832). The bacteria were grown on tryptic-soy agar (TSA) plates which were supplemented with 10ug/ml erythromycin or Kanamycin for the *Δlgt* mutant or the pRBlgt reconstituted strains, respectively. For preparation of bacteria colonies were picked and grown in 5ml tryptic-soy broth during vigorously shaking at 37ºC overnight (12-18hrs) for use in infection experiments. To prepare heat killed bacteria a pre-culture was diluted 1:100-200 in 50-100ml

tryptic-soy broth in 500-1000ml culture flasks and grown in a shaking-incubator to the exponential phase (approx. 4hrs), stationary phase (approx. 12hrs), or decline phase (20-24hrs), as appropriate. For heat killing of the bacteria was spun down, re-suspended in PBS, incubated at 80ºC for 30 minutes, and finally washed one time with PBS. For quantification of bacteria by OD-measurements a standard curve was generated with serial dilutions of heat killed (HK) bacteria that had been quantified by manual counting in a Bürker chamber. Fluorescent labelling of the HK bacteria was done using Alexa 488-succinimidyl-ester (SE) (Invitrogen). This reagent was dissolved in DMSO and immediately added to a solution of $2x10^{10}$ SA/ml in NaHCO3 (167uM, pH8.3) yielding a final concentration of 1mg/ml dye. Incubation with agitation was done for 1hr at RT, and the labelled bacteria were washed two times with 500ul PBS and counted. Preparation of crude bacterial lysate was done by a previous described protocol (4) with some modifications. Glass particles (0.1mm, Sigma) were pre-heated at 200ºC for 4 hours to eliminate potential TLR-ligand contaminants. The particles were added to $2x10^{10}$ SA113*Δlgt* (HK, exponential growth phase) in ice-cold PBS and run in four cycles on a Precellys 24 bead-beater (Bertin Technology, France) with chilling on ice between each cycle. The glass particles and intact bacteria were spun down and the crude lysate supernatants were added to new tubes for storage at -80ºC.

Blood, monocytes, and stimulation/infection

Fresh blood, serum, and buffycoats were acquired from healthy volunteers under informed written consent approved by the Regional Committee for Medical and Health Research Ethics (REC Central, Norway, #2009/2245). Human PBMC were isolated from buffycoats using Lymphoprep (Axis-Shield) as described by the manufacturer and monocytes were purified by adherence in culture plates and maintained in RPMI1640 (Gibco) supplemented with 10% pooled human serum. TLR2 blocking was done by 30 minutes pre-treatment with the anti-mouse/human TLR2 mAb clone T2.5 (#HM1054, Hycult Biotech) at 5ug/ml and mouse IgG1

mAb (R&D) served as isotype control. pI:C, pU, and crude SA lysate, with or without RNAse A (Qiagen) treatment (2ul/ml, 1hr at 37 ºC), was pre-complexed with pL-Arg at a 1:1 ratio (w/w) in Opti-MEM (Invitrogen), or with 2.5ul L2K/ug RNA in Opti-MEM for transfection. For infection of monocytes and macrophages live bacteria from overnight cultures with or without the bacterial culture media were diluted in RPMI and incubated for 1hr at RT before addition to the cells. Extracellular bacteria were killed after 1hr by addition of gentamycin to 100ug/ml. For Q-PCR analysis the cells were lysed after a total infection time of 3 to 4 hours, while cell culture supernatants were harvested after 5 to 6 hours of infection.

Macrophages, siRNA, and Q-PCR

Macrophages were derived from monocytes by differentiation in RPMI with 30% pooled human serum for 5-6 days. Medium was replaced with RPMI containing 10% serum for infection, stimulation or siRNA treatment. A pool of four individual ON-target Plus siRNAs (Dharmacon) was transfected using SilentFect (BioRad), yielding a final concentration of 5nM siRNA. The transfection was repeated after three days, and the silenced MDMs were infected with live SA for 3 hours. RNA was isolated with RNeasy kit including DNAse treatment (Qiagen), cDNA was transcribed with Maxima cDNA synthesis kit (Thermofisher), and relative quantification by realtime PCR (Q-PCR) was done with StepOne-plus using TaqMan probes (Life Technologies) and Perfecta Q-PCR fast-mix from Quanta. Probes used were: IFNβ: Hs01077958_s1, TNF: Hs00174128_m1, TLR7: Hs00152971_m1, TLR8: Hs00607866_mH, IRF5: Hs00158114_m1, STING: Hs00736958_m1, TBP: Hs00427620_m1. TBP served as endogenous control and relative expression in monocytes was calculated as fold induction by stimulation or infection. For siRNA treated macrophages the level of gene expression by infected cells were normalized against non-infected cells treated with each of the respective siRNAs to correct for potential background differences.

Whole blood model and flow cytometry analyses

The whole blood experiments were performed basically as described (23). Venous blood was drawn into polypropylene tubes with lepirudin (Refludan) anticoagulant (50ug/ml final concentration). The blood was quickly transferred to 1.8ml round bottomed cryotubes (Nunc) containing HK SA and FSL-1 and then incubated on a tube roller at 37ºC. Samples for cytokine analyses were centrifuged for collection of plasma, while samples for flow cytometry analyses were fixed immediately with 0.5% PFA for 5 minutes. For analysis of CD11b expression blood cells stimulated with HK bacteria and/or FLS-1 for 15 minutes were stained with anti-CD11b PE and anti-CD14 FITC (BD Biosciences) and Easylyse Erythrocyte Lysing Reagent (DAKO). Flow cytometry was performed on BD LSR II using SSC and CD14 to gate for neutrophils and monocytes, and CD11b-expression was determined by the median fluorescence intensity (MFI, PE) of the total cell distribution of monocytes and granulocytes. Phagocytosis of A488-labelled HK SA was analysed with the PhagoTest kit (BD Biosystems) according to the manufacturers instructions. In brief, full blood was incubated with bacteria with or without FSL-1 at 37 ºC for 30 minutes, while control tube with SA was kept on ice. Phagocytosis was stopped by placing tubes on ice and immediately adding ice-cold quenching solution. This was followed by washing with cold washing buffer, lysis of erythrocytes and fixation of leucocytes with lysis solution, and DNA stain was finally added to exclude artifacts of aggregated bacteria and cells. Monocytes and granulocytes were discriminated by FSC/SSC, and a "phagocytic index" (PI) was calculated as "mean fluorescence intensity (A488) of cells containing bacteria × fraction of cells containing bacteria".

Western blot

Cells were adhered in 6-well plates, treated and lysed in 150ul lysisbuffer (20mM Tris–HCl, 1mM EDTA, 1mM EGTA, 137mM NaCl, 1% Triton X-100, 1mM sodium deoxycholate, 10% glycerol, 1mM Na3VO4, 50mM NaF and Complete protease inhibitor (Roche)). PAGE

was performed with the NuPAGE system per the manufacturers (Life technologies) recommendations. Immunoblotting was performed with the iBlot system per the manufacturers (Life technologies) recommendations. After blotting, nitrocellulose membranes were briefly rinsed with dH20 and blocked with 5% BSA dissolved in TBS-T for one hour. All incubations with primary antibodies were done at 4^{o}C overnight, and all incubations with secondary HRP-linked antibodies (Dako #P0399 and #P0447) were done at room temperature for 1 hour. Blots were developed with Supersignal West Femto substrate (Pierce) and imaged with a Li-Cor Odyssey Fc system. Antibodies used for western blots in this study were: p38 (CST #9212), phospho-p38 (CST #9211), p44/42 (ERK, CST #4695), phospho-p44/42 (ERK, CST #4370), JNK (CST #9252), phospho-JNK (CST,#4668), TBK1 (CST #3504), phospho-TBK1 (CST #5483), phospho-IKKα/β (CST #2697), TAB1 (CST #3226), phospho-TAB1 (Millipore 06-1334), phospho-p105 (CST #4806), IkBα (CST #4812), GAPDH (Abcam ab8245), TLR8 (CST #11886), IRF5 (CST #13496).

Immunofluorescence and Scan^R analyses

Immunofluorescence labelling was done as described (9) with minor changes. PBMCs were seeded in 96-well glass bottom plates (#P96-1.5H-N, In Vitro Scientific, CA) which were pre-coated with human serum for 1-2 hrs. Non-adherent cells were removed by washing with 3 × HBSS. For intracellular staining the cells were fixed with ice-cold 2% paraformaldehyde (PFA) in PBS for 15 min on ice and washed 3 × with room tempered PBS. Permeabilization was done with PEM buffer (100 mM K-Pipes [pH 6.8], 5 mM EGTA, 2 mM $MgCl_2$, 0.05% saponin) for 10 min, quenched of free aldehyde groups in 50 mM NH_4Cl in PBS with 0.05% saponin (PBS-S) for 5 min, and blocked with 20% human serum (HS) in PBS-S for 20 min. After a single wash with 1%HS in PBS-S, the cells were incubated with primary antibody (2ug/ml) in with 1%HS in PBS-S overnight at 4°C. Cells were washed two times with room tempered PBS-S and once with 1%HS in PBS-S, and incubated with highly cross-adsorbed

Alexa Fluor 488 or 647-labeled secondary antibodies (Invitrogen) at 2ug/ml for 30 minutes. Subsequently the cells were washed with 3 × PBS-S, post-fixed with 4% PFA at room temperature, and washed once with PBS-S. Nuclei were stained with Hoechst-3342 (200ng/ml) in PBS-S. The following antibodies were used (typically 2-10ug/ml or 1:100-200 fold dilution): anti-human TLR8 (#NBP1-77203, Novus Biologicals), rabbit IgG Ctrl (NB810-56910, Novus Biologicals), anti-human IRF5 mAb (10T1, Abcam), anti-human IRF5 mAb (Abcam ab124792), anti-human IRF5 D10 (Santa Cruz), anti-human IRF5 (Sigma Aldrich HPA046700), anti-human IRF3 XP mAb (CST#11904), anti-human IRF3 mAb D83B9 mAb (CST#4302), anti-human IRF3 (Santa Cruz FL425, sc9082), anti-human p65 XP mAb (CST#8242), anti-human p65 A (Santa Cruz sc-109), anti-human IRF1 XP mAb (CST#8478), anti-human IRF7 (CST#4920; EPR4718 Abcam ab109255; H-246 Santa Cruz sc-9083), anti-phospho IRF7 (CST#5184), anti-human IRF8 (Santa Cruz, C-19 sc-6058; Sigma-Aldrich, HPA00253; CST#5628), normal goat IgG (Santa Cruz), rabbit IgG XP control mAb (CST). Automated imaging was done with the Scan^R system (Olympus) using a × 20 objective, up to 1 second exposure time, and approximately 100 frames were captured for each well (approx. 5.000-15.000 cells) performed in duplicates or triplicates. Automated image analysis was done with the Scan^R software v/1.3.0.3. Confocal images were captured with a Zeiss LSM 510 META scanning unit, and a 1.4 NA × 63 objective.

Statistical analyses

Statistical analyses were done on data merged from independent experiments, as indicated in the figures or the figure legends ("No. exp." or "n"). For analysis the data was log2-transformed to generate Gaussian distributions, and analyses were performed with GraphPad Prism v5.03. Figures without statistics are representative data from at least three independent experiments.

Results

SA inhibits the induction of IFNβ in human blood monocytes via TLR2 activation. To clarify the role of TLR2 ligands in SA-induced IFNβ production we infected monocytes with live SA 113 wild-type (wt) strain and its isogenic mutant 113-*Δlgt*. The mutant strain is deficient in mature lipoprotein production and fails to activate TLR2 resulting in impaired immune-activation by entire bacteria (4, 24). To examine the total immunostimulatory capacity of the different strains, we included both the bacteria and the supernatants from the bacterial cultures, and the plasmid-reconstituted 113-*Δlgt* strain (pRBlgt) served as a genotype/phenotype control (Fig. 1A). Unexpectedly the *Δlgt* strain induced higher levels of IFNβ than the wt and pRBlgt strains, suggesting that SA lipoproteins inhibit IFNβ induction by the bacteria. To examine the possible contribution of factors in the bacterial culture supernatant for this phenomenon the wt and *Δlgt* supernatants were swapped (Fig. 1B). This resulted in increased IFNβ-induction by the wt strain and concomitant increased IFNβ-induction by the mutant strain, thus reaching intermediate IFNβ-levels compared to the condition in Fig. 1A. This indicates that the SA 113-wt strain inhibit IFNβ induction by lipoproteins which are released into the bacterial culture media during growth, as well as by lipoproteins in the bacterial cell wall. Release of lipoproteins by the 113-wt strain during growth has been demonstrated previously (4), and with a TLR2-HEK293-NF-kB reporter assay we identified TLR2 ligands in the culture supernatant of the 113-wt strain, but not the *Δlgt* strain (not shown). To examine if TLR2-ligands of SA antagonize the induction of IFNβ during infection we used a TLR2-blocking antibody (Fig. 1C). In the presence of bacterial culture media the TLR2-blocing antibody increased the production of IFNβ by monocytes upon infection of all the SA strains examined, except for the 113- *Δlgt* strain. In the absence of bacterial culture media TLR2-blocking significantly increased the IFNβ production by the pathogenic SA isolates Newman and Cowan, with a similar tendency for the 113-wt and

Wood46 strains. Altogether this suggests that both lipoproteins released into the bacterial culture media and in the bacterial cell wall can antagonize the IFNβ production from monocytes via activation of TLR2. We further examined the role of TLR2 in the induction of other cytokines using multiplex ELISA. Secretion of IL6, IL8, IL1α and IL12-p40 by monocytes in response to SA infection was partially lipoprotein dependent, while secretion interleukin (IL)1β and IL18 was independent of lipoproteins (Fig. S1). Lipoproteins suppressed IL12p70 secretion to a similar degree as IFNβ, suggesting that these two cytokines share a regulatory mechanism (Fig. S1).

TLR2 ligands antagonize the induction of IFNβ by SA in human blood monocytes and whole blood. To simplify our model system we examined whether the defined synthetic TLR2/6 ligand FSL-1 alone would antagonize IFNβ-induction by HK SA *Δlgt*, *E. coli* and *E. coli* LPS (Fig. 2A). TLR2 co-stimulation with FSL-1 suppressed IFNβ induction by HK SA, but not HK *E. coli* and *E. coli* LPS. This confirmed that TLR2 activation blocks SA-induced IFNβ production, while it does not affect TLR4-TRIF signaling. Since SA lipopeptides can be both diacylated and triacylated (25), and synthetic triacylated TLR1/2 ligand Pam3Cys which also inhibited the IFNβ induction by HK SA in monocytes (not shown).

We further examined the impact of the timing of TLR2 ligand administration relative to SA and found that maximum inhibition of IFNβ-induction was achieved when FSL-1 was added before or at the same time as the bacteria, while the inhibitory effect was gradually reduced if FSL-1 was added 15, 30, and 60 minutes later (Fig. 2B). Thus, the TLR2-inhibitory effect is limited to an early time-frame of SA sensing by monocytes.

To examine if the inhibitory effect of TLR2 also is important in the more complex physiological environment of blood monocytes, we employed a lepirudin anti-coagulated human whole blood model (*ex vivo*) which enables crosstalk between all blood cells and most of the plasma cascades, including a C system that is functionally active under physiological

conditions (23). TLR2 co-stimulation fully suppressed SA-induced IFNβ production in whole blood (Fig. 2C) confirming the validity of our PBMC-based model. Cytokine induction by HK SA is to a large extent dependent on phagocytosis and bacterial degradation (20, 26). The TLR2 effect could thus possibly be explained by inhibition of phagocytosis. However, we found that TLR2 co-stimulation did not inhibit phagocytosis, but instead significantly increased the uptake of HK SA by monocytes in whole blood (Fig. 2E). The mechanism for the enhanced phagocytosis is likely TLR2-mediated activation of the CR3 (CD11b/CD18), as SA phagocytosis in the whole blood model is strongly C dependent (27) and the CD11b level on both monocytes and granulocytes increased strongly upon TLR2 stimulation (Fig. 2F).

SA RNA is an endosomal PRR ligand. As bacterial nucleic acids are implicated in type I IFN induction in various model systems, we examined the importance of RNA in crude lysate of the HK SA *Δlgt* strain. Bacteria were mechanically disrupted, treated with RNAse A which cleaves single-stranded RNA, and the lysate mixed with poly-L-Arginine (pL-Arg) for delivery of nucleic acid to the monocyte endosomal compartment (28) (Fig. 3). RNAse-treatment eliminated the induction of IFNβ, IL12p40, and IL12p70, and strongly reduced the release of IL1α, IL1β, and IL18. In contrast the levels of IL6 and IL8 were not affected by RNAse A (Fig. 3). This demonstrates that in lysate of HK SA deprived of TLR2 ligands ssRNA was a dominant PAMP for the induction of IFNβ, IL1, IL12, and IL18. Still, other PAMS distinct from RNA and lipoproteins were apparently dominating for IL6 and IL8 induction by these crude lysates.

TLR2 inhibits IFNβ and IL12 induction by both SA and TLR8 ligands. To clarify the mechanism of how SA RNA induces IFNβ in monocytes we compared the response by HK SA *Δlgt* with the synthetic TLR8-ligand polyuridylic acid (pU) and the dsRNA TLR3-ligand polyinosine:cytosine (pI:C). The RNA was delivered to the endosomal or the cytosolic

compartment of monocytes by complexation with pL-Arg or transfection with lipofectamine (L2K), respectively, as previously shown (28). Stimulation with SA, pU/pL-Arg, and pI:C/L2K induced IFNβ production, while stimulation with pI:C/pL-Arg and pU/L2K did not (Fig. 4A). This implies that pU and pI:C induces IFNβ from the endosomal and the cytosolic compartments, respectively, and is consistent with high TLR8- and low TLR3-levels in monocytes (29). Co-stimulation with FSL-1 strongly suppressed IFNβ induction by HK SA and pU, but not pI:C. TLR2 activation thus interferes with TLR8-signaling, but not cytosolic dsRNA-sensing or TLR4-TIR-domain containing adapter inducing IFNβ signaling (Fig. 2A). Moreover, induction of IL12-p70 was solely induced by SA and pU in endosomes and was also inhibited by TLR2-activation (Fig. 4B). GU- and U-rich ssRNA stimulate murine TLR7 and human TLR8 (30), and the induction of IL12-p70 is a well-described characteristics of human TLR8 (28, 31). Thus, the regulation of IFNβ and IL12-p70 production by monocytes is similar for SA and a defined TLR8-ligand, including its inhibition by TLR2-activation. Additional correlative evidence for the involvement of TLR8 in the sensing of SA was found using the TLR8 specific imidazoquinoline agonist CL75, as CL75 mediated IFNβ induction was antagonized by TLR2 co-stimulation (Fig. 4C). In contrast, IFNβ induction by the TLR7 specific ligand R837 was not antagonized by TLR2 co-stimulation (Fig. 4D), arguing against a role of TLR7 in the IFNβ induction by SA. TLR8 immunofluorescence indicated that TLR8 was recruited to SA phagosomes (Fig. 4E). Quantification using a high content screening system suggested that approximately 9% of the SA phagosomes stained positive for TLR8 one hour after exposure to bacteria (Fig. 4F).

SA induces IFNβ via TLR8 and IRF5

The correlative data suggested that TLR8 was responsible for SA-induced IFNβ production. Western blot analysis demonstrated that although SA and TLR2 ligands activated TBK1 phosphorylation, IRF3 was not activated (not shown). Furthermore, preliminary data

suggested a possible involvement of IRF5. To clarify the mechanism we performed gene silencing of MDMs by transient transfection with siRNA targeting TLR7, TLR8, IRF5, and Stimulator of interferon genes (STING). All targets were efficiently and specifically silenced on the mRNA level after sequential transfections (Fig. S2A). Clear knockdown of TLR8 and IRF5 was also seen at the protein level (Fig. S2B). However, two TLR8-bands of around 100kDa were not completely eliminated even several days after mRNA knockdown. These bands probably correspond to N-terminal fragments of TLR8 after cleavage in endosomes and can be a functional PRR as recently shown (32). MDMs showed similar responses as monocytes, as co-stimulation with synthetic TLR2 ligand or SA lipoproteins strongly antagonized IFNβ induction by SA and synthetic TLR8 ligand (not shown). Infection of silenced MDMs with live SA *Δlgt* demonstrated that induction of IFNβ was dependent on TLR8 and IRF5, but not TLR7 or STING (Fig. 5). Induction of TNF followed a similar trend as IFNβ upon TLR8 and IRF5 silencing, but was not as strongly affected and reached statistically significance only for the TLR7+TLR8 combined knockdown. Altogether this indicates an essential role of a TLR8-IRF5 pathway in the induction of IFNβ by SA, which also may contribute to SA-induced TNF production by monocytes.

SA and TLR8-ligands induce IRF5 nuclear accumulation which is antagonized by TLR2 activation.

To further examine IRF5 activation we established a quantitative immunofluorescence method of transcription factor nuclear accumulation using high-content screening (Scan^R) (Fig. S3). Monocytes were stimulated with HK SA and TLR8 ligands and nuclear accumulation of total p65 (NF-kB/RelA), IRF3 (Fig. S3) and IRF5 (Fig. 6) was examined. The level of nuclear IRF5 was low in resting cells (Fig. 6A) and was strongly increased following pU/pL-Arg stimulation (Fig. 6B) and phagocytosis of HK SA *Δlgt* (Fig. 6D). FSL-1 co-stimulation clearly reduced the nuclear accumulation of IRF5 induced by both stimuli (Fig.

6C and 6E), which thus correlates with suppressed IFNβ and IL12 induction. Moreover, if SA was heat-inactivated during the stationary growth phase, the bacteria were markedly less potent as IFNβ inducers (not shown). The stationary phase SA did not induce IRF5 nuclear accumulation (Fig. 5F), thus again demonstrating a correlation of SA-induced IFNβ production and IRF5 nuclear accumulation in monocytes. Around 25% of the monocytes that had phagocytosed HK SA *Δlgt* stained positive for nuclear IRF5 (Fig. 5G). The frequency was strongly reduced by co-stimulation with FSL-1, as well as when HK SA from the stationary growth phase was used. Moreover, cells that did not phagocytosed bacteria - "SA bystanders" – did not have increased IRF5 nuclear accumulation. Thus, IRF5 nuclear accumulation was dependent on SA phagocytosis and not a result of paracrine signals. Correlation of IRF5 translocation and phagocytosis was also seen in a whole-well overview with SA phagocytosis and IRF5 nuclear staining being strongest around the well center (not shown). pU/pL-Arg stimulation activated IRF5 nuclear accumulation to a similar degree as SA uptake, and was also suppressed by FSL-1 co-stimulation, while FSL-1 or LPS alone did not activate IRF5 (Fig. 5H). In contrast, nuclear accumulation of p65 was seen with ligands for all three TLRs examined (Fig. 5I). Only LPS activated IRF3 nuclear translocation (Fig. 5J) which is consistent with the IRF3 phosphorylation pattern (not shown). IRF1 was constitutively localized to the nuclei in monocytes, while IRF7 and IRF8 antibodies gave no specific staining (not shown). We conclude that SA induces IRF5 nuclear accumulation in monocytes as a consequence of TLR8 activation, and is blocked by TLR2 signaling.

TLR8-induced nuclear accumulation of IRF5 is dependent on TAK1 and IKKβ, while nuclear accumulation of p65 is TAK1 independent. We further examined the requirement of central signaling components in the MyD88-pathway for TLR8-mediated IRF5 and p65 activation and TLR2-induced p65 activation. We quantified IRF5/p65 nuclear staining by two-color immunofluorescence (Fig. 7A-C). We then used well-characterized chemical

inhibitors of central signaling kinases to block monocyte signaling. To minimize possible problems of toxicity and secondary effects of the inhibitors we chose CL75 as TLR8 ligand, as CL75 elicits more rapid cytokine-induction than pU/pL-Arg and SA and thus limits the required incubation time with the inhibitors. Two structurally nonrelated inhibitors of TAK1 (5z-7-oxozeanol and NG-25) and IKKβ (IKKII-VIII and BI605906) were given as a 30 minute pre-treatment and their effects on TLR8- and TLR2-mediated nuclear accumulation of IRF5 and/or p65 were examined (Fig. 7D-F). TLR8-induced IRF5 nuclear accumulation was dependent on both TAK1 and IKKβ (Fig. 7D). In contrast, p65 nuclear accumulation following TLR8 and TLR2 stimulation was only dependent on IKKβ and not on TAK1 (Fig. 7E and 7F).

Western blot analysis of mitogen-activated protein kinases (MAPKs) and other signaling intermediates was performed to verify the specificity of the inhibitors and to dissect further details of TLR2 and TLR8 signaling (Fig. S4). Both TAK1 inhibitors effectively blocked TLR2- and TLR8-induced JNK and p38 phosphorylation, in contrast to the IKKβ inhibitors. IKKβ inhibitors still blocked the phosphorylation of p105 and ERK1/2. This is in agreement with the canonical model of MyD88-signaling were JNK and p38 are downstream of TAK1, while activation of p105 and ERK1/2 are controlled by IKKβ (33). The degradation of IkBα was not blocked by any of these inhibitors (Fig. S4) and IKKα can probably phosphorylate IkBα leading to its degradation once IKKβ is lost (34). Failure of TAK1-inhibitors to rescue IkBα from degradation fits with the TAK1 independent nuclear accumulation of p65 (Fig. 7E and F), while p65 activation may require phosphorylation by IKKβ in addition to degradation of IkBα (33). The TAK1 inhibitor 5z-7-oxozeanol efficiently antagonized IKKα/β phosphorylation and IKKβ activity (Fig. S4B), while NG25 was less efficient (Fig. S4A).

We further used gene silencing to examine the role of TLR7, TLR8, IRF5, IKKβ, STING, and TBK1 for IRF5 nuclear accumulation in MDMs upon infection with SA *Δlgt* (Fig. 7G). Silencing show that also in MDMs SA activates IRF5 via TLR8 and IKKβ, confirming the specificity of IRF5 staining and the inhibitor data, while TLR7, TBK1, STING and p65 silencing did not influence IRF5 activation. In contrast, p65 nuclear accumulation was reduced solely with siRNA for p65, verifying the specificity of the nuclear translocation assay also for this factor (Fig. 7H).

We conclude that both primary monocytes and MDMs sense SA via TLR8, and that TLR8-signaling includes a novel TAK1-IKKβ-IRF5 pathway which is required for IFNβ induction and which is blocked by TLR2 signaling. We thus propose a model for TLR8 and TLR2 signaling in monocytes that includes two distinct pathways (Fig. 8).

Discussion

We here provide evidence for a novel role of TLR8 in sensing of SA by human primary phagocytes. The physiological role of TLR8 is demonstrated by its contribution to the cytokine response induced by the whole bacteria during infection. While TLR2 and TLR8 display considerable redundancy in signaling and both contributed to SA-induced production of pro-inflammatory cytokines such as IL1α/β, IL18, and TNF, we show a specific role of TLR8 for the induction of IFNβ and IL12 via IRF5 activation. TLR8 and IRF5 also contributed to TNF-production. It is possible that IFNR-signaling could have influenced the TNF response, this seems less likely given the short incubation time (3hrs) used.

The function of human TLR8 as a sensor of bacterial RNA appears similar as murine TLR13 (13, 14). However, while TLR13 detects a short sequence of bacterial 23S RNA with high specificity (14, 35), TLR7 and TLR8 have weak sequence specificity and generally detects U-rich RNA (30). Recently it was found that the natural TLR8 ligands are degradation products of U-rich RNA in the form of uridine and short U-containing oligomers that work synergistically (36). In agreement with this model the commercial TLR13-ligand Sa19, which has a single U residue and is stabilized by thioester backbone, did not activate human monocytes or TLR8-expressing HEK293 cells (not shown). Thus, while human TLR8 and murine TLR13 may seem functionally analogous, their ligand specificities and mechanisms of activation are different.

The role of IFNβ in SA pathogenesis is controversial, and two recent studies found contradictory effects of IFNβ on the outcome of experimental murine infection (19, 20). In humans SA forms abscesses with a high local bacterial load which can leak into the surrounding tissue and the blood stream. The maximum levels of IFNβ produced in response to HK SA exceeded that of HK *E. coli* and LPS. A more potent induction of IFNβ by HK SA from the exponential phase than the stationary phase may be related to the change in cell-wall

thickness (37), or it could reflect changes in the amount of stimulatory RNA. Only a fraction (e.g. 20-30%) of the monocyte population stained positive for IRF5 and IRF3 nuclear accumulation after TLR8 or TLR4 activation, respectively. This fits with a stochastic model of IFNβ production in a cell population, which is explained by variations in limiting components at the cellular level (38, 39). TLR8 is also a potent inducer of IL12 in human monocytes (28, 31), while IRF5 regulates macrophage polarization and drives IL12 and IL23 production and T-helper-1 (Th1)-Th17 activation (40). Th17-cells may also be important for protection from SA infections (41). We found that lipoproteins of SA, either soluble or in the bacterial cell wall, activated TLR2 and strongly suppressed TLR8-induced production of IFNβ and IL12 by bacteria being degraded in phagosomes. This may represent a control mechanism to limit IFNβ and IL12 production induced by extracellular bacteria. It is thus possible that dysregulation of TLR2/TLR8 signaling can lead to disease progression, and it could represent a new immune-evasion target for bacteria such as SA.

Human blood monocytes also sense *B. burgdorferi* (Bb) RNA via TLR8 resulting in IFNβ production (42, 43). While this finding is in agreement with our present study on SA, the proposed signaling mechanisms are different as they suggested IRF7 to be the central transcription factor involved. We show that TLR8-induced IFNβ production in monocytes and MDMs is dependent on IRF5. The activation of IRF5 by SA and TLR8 ligands was rapid and did not occur in bystander cells not infected by SA, excluding the possibility that IRF5 is triggered via a secondary mediator. *M. tuberculosis* induces IFNβ in mouse macrophages through a NOD2-RIP2-TBK1-IRF5 pathway (44). Also, a NOD2-IRF5 mechanism of SA-mediated IFNβ induction in mouse BMDCs was recently reported (45), and IRF5 was activated by TBK1/IKKi and RIP2 in overexpression studies (46, 47). However, we found no induction of IFNβ in RNA-depleted SA lysates, which most likely contain significant amounts of peptidoglycan and bacterial cell-wall fragments. Moreover, silencing of TBK1 in

MDMs did not affect IRF5 translocation in our studies. Thus, neither NOD2 nor TBK1 seems to be involved in SA-mediated IRF5 activation, arguing against a NOD2-RIP2-TBK1 pathway for SA-induced IFNβ in primary human phagocytes.

In model systems TLR7 and TLR8 can activate both IRF5 and IRF7, but not IRF3, and in THP-1 monocytic cells TLR7-induced IFNα is IRF5 dependent (47). In human pDCs, IRF5 rather than IRF7 regulates TLR9-induced IFNβ production together with NF-κB p50 (48). It thus appears that TLR7-, TLR8-, and TLR9-signaling can involve IRF5 in different cell types. IFN-type I induction by TLR7 and TLR9 in the human pDC cell line Gen2.2 is dependent of TAK1 and IKKβ, but independent on IRF7 (34), which is similar to our findings of TLR8-induced IFNβ in primary phagocytes. An essential function of IRF5 for IFNβ induction by TLR7 ligands in Gen2.2 cells was recently demonstrated by Cohen et al. (49). They found that IKKβ catalyzes IRF5 phosphorylation leading to its dimerization and nuclear translocation resulting in induction of IFNβ and IL12, but not IL6. Our finding on TLR8-induced signaling in human primary monocytes and MDMs is similar to this newly described TLR7-TAK1-IKKβ-IRF5-IFNβ pathway in Gen2.2 cells. The function of IKKβ as a kinase activating IRF5 was confirmed by another study (50). Our study using human primary monocytes and MDMs stimulated with live SA captures a more physiological relevant function of this recently identified IKKβ-IRF5 link. Additionally, we demonstrate a regulatory role of TLR2 in this pathway in primary cells.

The function of TAK1 is cell-type dependent (51) and was not necessary for p65/RelA nuclear accumulation in monocytes in our study. A TAK1 independent but MEKK3 dependent pathway of NF-κB activation has been described in mouse and human model systems (52, 53) and could possibly be involved also in human primary monocytes.

Monocytes have high mRNA levels of TLR2, TLR4 and TLR8, and low levels of TLR3, TLR7 and TLR9 (29), which is generally in agreement with our data. Still, the TLR7-

specific ligand (R837) induced IFNβ production in monocytes, suggesting that TLR7 is expressed at a functional level. The differential abilities of TLR8 and TLR2 to activate IRF5 via MyD88 might be related to their predominant localization within different cellular compartments - endosomal versus cell surface. TLR2 did not inhibit IFNβ induction via TLR4-, TLR7- or cytosolic pI:C which indicate a specificity for TLR8 signaling by TLR2 suppression. It is unclear whether the TLR2-induced feedback mechanism targets IRF5 directly, or if it acts upstream and interferes more generally with TLR8 signaling. Distinct signaling pathways activated by TLR2 that inhibition TLR8 signaling is a subject of future studies.

In conclusion, we have identified TLR8 as physiological significant sensor of entire SA and described a novel TLR8-IRF5 signaling axis triggering IFNβ production in primary human monocytes and macrophages antagonized by TLR2. This mechanism may be important for the sensing of infection with SA and possibly other pyogenic bacteria, thus providing new possible targets for pharmacological immunomodulation in conditions such as Gram-positive sepsis.

Acknowledgements

The imaging was performed at the Cellular & Molecular Imaging Core Facility (CMIC), Norwegian University of Science and Technology (NTNU). Thanks to Dionne Klein and Kjartan Egeberg at CMIC for technical assistance with imaging, and to Dorte Christansen for help with flow cytometry.

Conflicts of interest

The authors declare no competing financial interests.

References

1. Anwar, S., L. R. Prince, S. J. Foster, M. K. B. Whyte, and I. Sabroe. 2009. The rise and rise of Staphylococcus aureus: laughing in the face of granulocytes. *Clin. Exp. Immunol.* 157: 216–24.

2. Foster, T. J. 2005. Immune evasion by staphylococci. *Nat. Rev. Microbiol.* 3: 948–58.

3. Takeuchi, O., K. Hoshino, and S. Akira. 2000. Cutting edge: TLR2-deficient and MyD88-deficient mice are highly susceptible to Staphylococcus aureus infection. *J. Immunol.* 165: 5392–6.

4. Stoll, H., J. Dengjel, C. Nerz, and F. Gotz. 2005. Staphylococcus aureus deficient in lipidation of prelipoproteins is attenuated in growth and immune activation. *Infect. Immun.* 73: 2411–2423.

5. Von Bernuth, H., C. Picard, Z. Jin, R. Pankla, H. Xiao, C.-L. Ku, M. Chrabieh, I. Ben Mustapha, P. Ghandil, Y. Camcioglu, J. Vasconcelos, N. Sirvent, M. Guedes, A. B. Vitor, M. J. Herrero-Mata, J. I. Aróstegui, C. Rodrigo, L. Alsina, E. Ruiz-Ortiz, M. Juan, C. Fortuny, J. Yagüe, J. Antón, M. Pascal, H.-H. Chang, L. Janniere, Y. Rose, B.-Z. Garty, H. Chapel, A. Issekutz, L. Maródi, C. Rodriguez-Gallego, J. Banchereau, L. Abel, X. Li, D. Chaussabel, A. Puel, and J.-L. Casanova. 2008. Pyogenic bacterial infections in humans with MyD88 deficiency. *Science* 321: 691–6.

6. Von Bernuth, H., C. Picard, A. Puel, and J.-L. Casanova. 2012. Experimental and natural infections in MyD88- and IRAK-4-deficient mice and humans. *Eur. J. Immunol.* 42: 3126–35.

7. Decker, T., M. Müller, and S. Stockinger. 2005. The yin and yang of type I interferon activity in bacterial infection. *Nat. Rev. Immunol.* 5: 675–87.

8. Kagan, J. C., T. Su, T. Horng, A. Chow, S. Akira, and R. Medzhitov. 2008. TRAM couples endocytosis of Toll-like receptor 4 to the induction of interferon-beta. *Nat. Immunol.* 9: 361–8.

9. Husebye, H., M. H. Aune, J. Stenvik, E. Samstad, F. Skjeldal, O. Halaas, N. J. Nilsen, H. Stenmark, E. Latz, E. Lien, T. E. Mollnes, O. Bakke, and T. Espevik. 2010. The Rab11a GTPase controls Toll-like receptor 4-induced activation of interferon regulatory factor-3 on phagosomes. *Immunity* 33: 583–96.

10. Deshmukh, S. D., B. Kremer, M. Freudenberg, S. Bauer, D. T. Golenbock, and P. Henneke. 2011. Macrophages recognize streptococci through bacterial single-stranded RNA. *EMBO Rep.* 12: 71–6.

11. Mancuso, G., M. Gambuzza, A. Midiri, C. Biondo, S. Papasergi, S. Akira, G. Teti, and C. Beninati. 2009. Bacterial recognition by TLR7 in the lysosomes of conventional dendritic cells. *Nat. Immunol.* 10: 587–594.

12. Gratz, N., H. Hartweger, U. Matt, F. Kratochvill, M. Janos, S. Sigel, B. Drobits, X.-D. Li, S. Knapp, and P. Kovarik. 2011. Type I interferon production induced by Streptococcus pyogenes-derived nucleic acids is required for host protection. *PLoS Pathog.* 7: e1001345.

13. Hidmark, A., A. von Saint Paul, and A. H. Dalpke. 2012. Cutting edge: TLR13 is a receptor for bacterial RNA. *J. Immunol.* 189: 2717–21.

14. Oldenburg, M., A. Krüger, R. Ferstl, A. Kaufmann, G. Nees, A. Sigmund, B. Bathke, H. Lauterbach, M. Suter, S. Dreher, U. Koedel, S. Akira, T. Kawai, J. Buer, H. Wagner, S. Bauer, H. Hochrein, and C. J. Kirschning. 2012. TLR13 recognizes bacterial 23S rRNA devoid of erythromycin resistance-forming modification. *Science* 337: 1111–5.

15. Kasahara, T., H. Harada, H. Wakasugi, M. Imai, M. Mayumi, T. Santo, and A. Sugiura. 1982. Potentiation of natural killer cell activity of human lymphocytes in vitro: the participation of interferon in stimulation with Staphylococcus aureu Cowan I bacteria but not with Protein A. *Immunology* 45: 687–695.

16. Smith, E. M., H. M. Johnson, and J. E. Blalock. 1983. Staphylococcus-Aureus Protein A Induces the Production of Interferon-Alpha in Human-Lymphocytes and Interferon-Alpha-Beta in Mouse Spleen-Cells. *J. Immunol.* 130: 773–776.

17. Svensson, H., B. Cederblad, M. Lindahl, and G. Alm. 1996. Stimulation of natural interferon-alpha beta-producing cells by Staphylococcus aureus. *J. Interf. Cytokine Res.* 16: 7–16.

18. Martin, F. J., M. I. Gomez, D. M. Wetzel, G. Memmi, M. O'Seaghdha, G. Soong, C. Schindler, and A. Prince. 2009. Staphylococcus aureus activates type I IFN signaling in mice and humans through the Xr repeated sequences of protein A. *J. Clin. Invest.* 119: 1931–1939.

19. Parker, D., and A. Prince. 2012. Staphylococcus aureus Induces Type I IFN Signaling in Dendritic Cells Via TLR9. *J. Immunol.* 189: 4040–46.

20. Kaplan, A., J. Ma, P. Kyme, A. J. Wolf, C. A. Becker, C. W. Tseng, G. Y. Liu, and D. M. Underhill. 2012. Failure To Induce IFN-β Production during Staphylococcus aureus Infection Contributes to Pathogenicity. *J. Immunol.* 189: 4537–45.

21. Liljeroos, M., R. Vuolteenaho, S. Rounioja, B. Henriques-Normark, M. Hallman, and M. Ojaniemi. 2008. Bacterial ligand of TLR2 signals Stat activation via induction of IRF1/2 and interferon-alpha production. *Cell. Signal.* 20: 1873–81.

22. Parcina, M., C. Wendt, F. Goetz, R. Zawatzky, U. Zahringer, K. Heeg, and I. Bekeredjian-Ding. 2008. Staphylococcus aureus-Induced Plasmacytoid Dendritic Cell Activation Is Based on an IgG-Mediated Memory Response. *J. Immunol.* 181: 3823–3833.

23. Mollnes, T. E., O. L. Brekke, M. Fung, H. Fure, D. Christiansen, G. Bergseth, V. Videm, K. T. Lappegard, J. Kohl, and J. D. Lambris. 2002. Essential role of the C5a receptor in E-coli-induced oxidative burst and phagocytosis revealed by a novel lepirudin-based human whole blood model of inflammation. *Blood* 100: 1869–1877.

24. Wardenburg, J. B., W. A. Williams, and D. Missiakas. 2006. Host defenses against Staphylococcus aureus infection require recognition of bacterial lipoproteins. *Proc. Natl. Acad. Sci. U. S. A.* 103: 13831–13836.

25. Kurokawa, K., M.-S. Kim, R. Ichikawa, K.-H. Ryu, N. Dohmae, H. Nakayama, and B. L. Lee. 2012. Environment-mediated accumulation of diacyl lipoproteins over their triacyl counterparts in Staphylococcus aureus. *J. Bacteriol.* 194: 3299–306.

26. Ip, W. K. E., A. Sokolovska, G. M. Charriere, L. Boyer, S. Dejardin, M. P. Cappillino, L. M. Yantosca, K. Takahashi, K. J. Moore, A. Lacy-Hulbert, and L. M. Stuart. 2010. Phagocytosis and Phagosome Acidification Are Required for Pathogen Processing and MyD88-Dependent Responses to Staphylococcus aureus. *J. Immunol.* 184: 7071–7081.

27. Skjeflo, E. W., D. Christiansen, T. Espevik, E. W. Nielsen, and T. E. Mollnes. 2014. Combined inhibition of complement and CD14 efficiently attenuated the inflammatory response induced by Staphylococcus aureus in a human whole blood model. *J. Immunol.* 192: 2857–64.

28. Ablasser, A., H. Poeck, D. Anz, M. Berger, M. Schlee, S. Kim, C. Bourquin, N. Goutagny, Z. Jiang, K. A. Fitzgerald, S. Rothenfusser, S. Endres, G. Hartmann, and V. Hornung. 2009. Selection of molecular structure and delivery of RNA oligonucleotides to activate TLR7 versus TLR8 and to induce high amounts of IL-12p70 in primary human monocytes. *J. Immunol.* 182: 6824–33.

29. Hornung, V., S. Rothenfusser, S. Britsch, A. Krug, B. Jahrsdörfer, T. Giese, S. Endres, and G. Hartmann. 2002. Quantitative expression of toll-like receptor 1-10 mRNA in cellular subsets of human peripheral blood mononuclear cells and sensitivity to CpG oligodeoxynucleotides. *J. Immunol.* 168: 4531–7.

30. Heil, F., H. Hemmi, H. Hochrein, F. Ampenberger, C. Kirschning, S. Akira, G. Lipford, H. Wagner, and S. Bauer. 2004. Species-specific recognition of single-stranded RNA via toll-like receptor 7 and 8. *Science* 303: 1526–9.

31. Gorden, K. B., K. S. Gorski, S. J. Gibson, R. M. Kedl, W. C. Kieper, X. Qiu, M. a Tomai, S. S. Alkan, and J. P. Vasilakos. 2005. Synthetic TLR agonists reveal functional differences between human TLR7 and TLR8. *J. Immunol.* 174: 1259–68.

32. Ishii, N., K. Funami, M. Tatematsu, T. Seya, and M. Matsumoto. 2014. Endosomal Localization of TLR8 Confers Distinctive Proteolytic Processing on Human Myeloid Cells. *J. Immunol.* 193: 5118–28.

33. Clark, K., S. Nanda, and P. Cohen. 2013. Molecular control of the NEMO family of ubiquitin-binding proteins. *Nat. Rev. Mol. Cell Biol.* 14: 673–85.

34. Pauls, E., N. Shpiro, M. Peggie, E. R. Young, R. J. Sorcek, L. Tan, H. G. Choi, and P. Cohen. 2012. Essential role for IKKβ in production of type 1 interferons by plasmacytoid dendritic cells. *J. Biol. Chem.* 287: 19216–28.

35. Li, X.-D., and Z. J. Chen. 2012. Sequence specific detection of bacterial 23S ribosomal RNA by TLR13. *Elife* 1: e00102.

36. Geyer, M., K. Pelka, and E. Latz. 2015. Synergistic activation of Toll-like receptor 8 by two RNA degradation products. *Nat. Struct. Mol. Biol.* 22: 99–101.

37. Williams, I., F. Paul, D. Lloyd, R. Jepras, I. Critchley, M. Newman, J. Warrack, T. Giokarini, a J. Hayes, P. F. Randerson, and W. a Venables. 1999. Flow cytometry and other techniques show that Staphylococcus aureus undergoes significant physiological changes in the early stages of surface-attached culture. *Microbiology* 145: 1325–1333.

38. Zhao, M., J. Zhang, H. Phatnani, S. Scheu, and T. Maniatis. 2012. Stochastic expression of the interferon-β gene. *PLoS Biol.* 10: e1001249.

39. Rand, U., M. Rinas, J. Schwerk, G. Nöhren, M. Linnes, A. Kröger, M. Flossdorf, K. Kály-Kullai, H. Hauser, T. Höfer, and M. Köster. 2012. Multi-layered stochasticity and paracrine signal propagation shape the type-I interferon response. *Mol. Syst. Biol.* 8: 584.

40. Krausgruber, T., K. Blazek, T. Smallie, S. Alzabin, H. Lockstone, N. Sahgal, T. Hussell, M. Feldmann, and I. a Udalova. 2011. IRF5 promotes inflammatory macrophage polarization and TH1-TH17 responses. *Nat. Immunol.* 12: 231–8.

41. Proctor, R. a. 2011. Is there a future for a Staphylococcus aureus vaccine? *Vaccine* 30: 2921–2927.

42. Cervantes, J. L., C. J. La Vake, B. Weinerman, S. Luu, C. O'Connell, P. H. Verardi, and J. C. Salazar. 2013. Human TLR8 is activated upon recognition of Borrelia burgdorferi RNA in the phagosome of human monocytes. *J. Leukoc. Biol.* 94: 1231–41.

43. Cervantes, J. L., S. M. Dunham-Ems, C. J. La Vake, M. M. Petzke, B. Sahay, T. J. Sellati, J. D. Radolf, and J. C. Salazar. 2011. Phagosomal signaling by Borrelia burgdorferi in human monocytes involves Toll-like receptor (TLR) 2 and TLR8 cooperativity and TLR8-mediated induction of IFN-beta. *Proc. Natl. Acad. Sci. U. S. A.* 108: 3683–8.

44. Pandey, A. K., Y. Yang, Z. Jiang, S. M. Fortune, F. Coulombe, M. A. Behr, K. A. Fitzgerald, C. M. Sassetti, and M. A. Kelliher. 2009. NOD2, RIP2 and IRF5 play a critical role in the type I interferon response to Mycobacterium tuberculosis. *PLoS Pathog.* 5: e1000500.

45. Parker, D., P. J. Planet, G. Soong, A. Narechania, and A. Prince. 2014. Induction of type I interferon signaling determines the relative pathogenicity of Staphylococcus aureus strains. *PLoS Pathog.* 10: e1003951.

46. Chang Foreman, H.-C., S. Van Scoy, T.-F. Cheng, and N. C. Reich. 2012. Activation of Interferon Regulatory Factor 5 by Site Specific Phosphorylation. *PLoS One* 7: e33098.

47. Schoenemeyer, A., B. J. Barnes, M. E. Mancl, E. Latz, N. Goutagny, P. M. Pitha, K. a Fitzgerald, and D. T. Golenbock. 2005. The interferon regulatory factor, IRF5, is a central mediator of toll-like receptor 7 signaling. *J. Biol. Chem.* 280: 17005–12.

48. Steinhagen, F., A. P. McFarland, L. G. Rodriguez, P. Tewary, A. Jarret, R. Savan, and D. M. Klinman. 2013. IRF-5 and NF-κB p50 co-regulate IFN-β and IL-6 expression in TLR9-stimulated human plasmacytoid dendritic cells. *Eur. J. Immunol.* 43: 1896–906.

49. Lopez-Pelaez, M., D. J. Lamont, M. Peggie, N. Shpiro, N. S. Gray, and P. Cohen. 2014. Protein kinase IKKβ-catalyzed phosphorylation of IRF5 at Ser462 induces its dimerization and nuclear translocation in myeloid cells. *Proc. Natl. Acad. Sci. U. S. A.* 111: 17432–7.

50. Ren, J., X. Chen, and Z. J. Chen. 2014. IKKβ is an IRF5 kinase that instigates inflammation. *Proc. Natl. Acad. Sci. U. S. A.* 111: 17438–43.

51. Ajibade, A. a, H. Y. Wang, and R.-F. Wang. 2013. Cell type-specific function of TAK1 in innate immune signaling. *Trends Immunol.* 34: 307–316.

52. Qin, J., J. Yao, G. Cui, H. Xiao, T. W. Kim, J. Fraczek, P. Wightman, S. Sato, S. Akira, A. Puel, J.-L. Casanova, B. Su, and X. Li. 2006. TLR8-mediated NF-kappaB and JNK activation are TAK1-independent and MEKK3-dependent. *J. Biol. Chem.* 281: 21013–21.

53. Zhou, H., M. Yu, K. Fukuda, J. Im, P. Yao, W. Cui, K. Bulek, J. Zepp, Y. Wan, T. W. Kim, W. Yin, V. Ma, J. Thomas, J. Gu, J. Wang, P. E. DiCorleto, P. L. Fox, J. Qin, and X. Li. 2013. IRAK-M mediates Toll-like receptor/IL-1R-induced NFκB activation and cytokine production. *EMBO J.* 32: 583–96.

Figure legends

Fig. 1. *S. aureus* (SA)-infected blood monocytes produce IFNβ which can be antagonized by secreted lipoproteins via TLR2. Monocytes were infected with SA 113 wt strain, its isogenic *lgt*-mutant (*Δlgt*), or the plasmid-reconstituted *Δlgt* strain (pRBlgt). Extracellular bacteria were killed with gentamycin after 1hr and cell-culture supernatant was sampled 5 to 6hrs later. (A) Dose dependent induction of IFNβ with SA including the bacterial culture supernatant 'S'. (B) Effect of swapping supernatants of the *Δlgt* and wt bacterial cultures on the induction of IFNβ. The IFNβ levels from triplicates were determined by ELISA (mean ±SD). (C) The effect of the TLR2-blocking mAb (T2.5, 5ug/ml) on the IFNβ production induced by infection with different SA strains ($1x10^8$/ml) with or without inclusion of the bacterial culture supernatants (mean + SEM, n=4). Differences were tested by 2way RM ANOVA with Bonferroni posttest. *$p < 0.05$, **$p < 0.01$, ***$p < 0.001$.

Fig. 2. Synthetic TLR2-ligand inhibits SA-induced production of IFNβ in human monocytes and whole blood, but enhances phagocytosis. Monocytes were co-stimulated

with TLR2 ligand (FSL-1) and heat killed (HK) bacteria or LPS for 6hrs. (A) Effect of FSL-1 (1, 10, and 100ng/ml) co-treatment on IFNβ induction with HK *E. coli* (K12 strain, $1x10^7$/ml), *E. coli* LPS (K12, 100ng/ml), and HK SA *Δlgt* ($1x10^8$/ml). (B) Effect of timing of administration of FSL-1 (10ng/ml) relative to HK SA *Δlgt* ($1x10^8$/ml). The IFNβ levels from triplicates were determined by ELISA (mean ±SD). (C) FSL-1 inhibits induction of IFNβ by HK SA *Δlgt* ($1x10^9$/ml) in a human whole blood model (3hrs, mean +SEM, n=3). The effect of FSL-1 co-stimulation was tested by 1way RM ANOVA with Dunnett's Multiple Comparison Test. (D) Effect of FSL-1 co-stimulation on phagocytosis of HK SA in human whole blood (30min., mean +SEM, n=3). The effect of FSL-1 co-stimulation was tested with two-way paired t-test. (E) Effect of SA, FSL-1 and co-stimulation on the CD11b/CD18 surface level on phagocytes in human whole blood (30 min., mean +SEM, n=3). The effect of FSL-1 co-stimulation was tested by 1way RM ANOVA with Bonferroni's Multiple Comparison Test. *$p < 0.05$, **$p < 0.01$, ***$p < 0.001$.

Fig. 3. SA RNA induces IFNβ, IL12, IL1, and IL18, but is redundant for induction of IL6 and IL8 in monocytes. Homogenate of HK SA *Δlgt* were made by mechanical disruption using glass particles and a bead-beater. The lysate was subsequently treated with or without RNAse A for 1hr at 37°C. The crude lysate was delivered to the monocytes as a complex with cationic protein (pL-Arg) and supernatants after 6hrs of treatment were assayed for cytokines using ELISA (IFNβ) and BioPlex (mean +SD of triplicates).

Fig. 4. SA and TLR8-ligand induced IFNβ and IL12 is antagonized by TLR2-activation. Monocytes were stimulated with HK SA *Δlgt* (10^8/ml), ssRNA (pU, 0.75ug/ml), and dsRNA (pI:C, 0.75ug/ml), and with or without FSL-1 co-stimulation (10ng/ml). The synthetic RNA was delivered as a complex with pL-Arg or cationic lipid (L2K) to examine the stimulatory effect of RNA in the endosomal (pL-Arg) versus the cytosolic (L2K) compartment. After 6hrs

the supernatants were sampled and assayed for (A) IFNβ and (B) IL12p70 (mean +SD of triplicates). (C, D) Monocytes were stimulated for with TLR8 specific ligand (CL75) or TLR7 specific ligand (R837) with or without FSL-1 co-administration (100ng/ml) for 2hrs (mean ±SEM, n=3). The differences were tested by 2way RM ANOVA with Bonferroni posttest. ***p< 0.001. (E-F) Monocytes were treated for 1hr with Alexa488-labelled HK SA Δ*lgt* ($1x10^8$/ml), then fixed and stained with (D) anti-TLR8 and (E) control Abs. (F) Quantification of the percentage of TLR8-positive SA phagosomes using high-content screening analysis (Scan^R). Nuclei are stained with Hoechst (blue). Scalebar = 10um.

Fig. 5. SA induces IFNβ production via TLR8 and IRF5 in MDMs. Monocyte-derived macrophages (MDMs) were treated with siRNA as indicated. Infection with live SA Δ*lgt* ($3x10^7$/ml) including bacterial culture medium was done for 3hrs and the fold induction of IFNβ and TNF expression by infection was determined with RT/Q-PCR (mean +SEM, n=4). The effect of silencing was tested by 1way RM ANOVA with Dunnett's Multiple Comparison Test compared to Ctrl siRNA. *p<0.05, **p<0.01, ***p<0.001.

Fig. 6. SA and pU/pL-Arg complexes induce nuclear accumulation of IRF5 in monocytes, but not IRF3. (A-F) Monocytes were treated for 2-4hrs with pU/pL-Arg (7.5ug/ml) and Alexa488-labelled HK SA Δ*lgt* ($1x10^8$/ml) from exponential and stationary growth phases, respectively, and with or without FSL-1 (10ng/ml) co-stimulation. Subsequently the cells were fixed and immunostained for IRF5 and automated imaging and analyses of nuclear IRF5 accumulation was done with Scan^R. (A) IRF5 staining in monocyte without stimulation, (B) with pU/pL-Arg, (C) with pU/pL-Arg + FSL-1, (D) with HK SA from exponential growth phase, (E) with HK SA + FSL-1, (F) with HK SA from stationary growth phase. (G-H) The frequencies of cells showing positively stained for IRF5 was determined from approximately 5000-15000 cells (100 frames per well). (G) Frequencies of

IRF5 positive nuclei among monocytes having phagocytosed HK SA harvested during the exponential growth phase; the effect of FSL-1 co-stimulation; monocytes having phagocytosed HK SA harvested during the stationary growth phase; monocytes in wells with HK SA from the exponential growth phase, but which have not taken up bacteria ('SA bystanders'). (H-J) Monocytes were stimulated with pU/pL-Arg with or without FSL-1 for 4hrs, or with FSL-1 (10ng/ml) and E. coli K12 LPS (100ng/ml) alone for 1hr. The cells were fixed and stained with antibodies for (H) total IRF5, (I) total p65 (NF-κB subunit RelA) and (J) IRF3, and the frequencies of positively stained nuclei were determined (mean +SD of duplicates and triplicates). Scalebar = 20 um.

Fig. 7. TLR8-induced IRF5 nuclear accumulation is dependent on TAK1 and IKKβ, while TLR8- and TLR2-induced p65 nuclear accumulation is IKKβ dependent but TAK1 independent. Monocytes were stimulated with CL75 (1ug/ml) and FSL-1 (10ng/ml) for 1hr, then fixed and stained for IRF5 and p65 by immunofluorescence. Imaging and quantification of IRF5 and p65 positive nuclei was done with Scan^R. (A) IRF5 and p65 double-stained cells without stimulation. (B) IRF5 and p65 double-stain cells after CL75 stimuli. (C) Analysis of nuclear p65 and IRF5 staining intensity (mean fluorescence) after CL75 stimulation. (D-F) Effect of pharmacological inhibitors of TAK1 and IKKβ on nuclear accumulation of IRF5 and p65 following CL75 and FSL-1 stimulation. (D) Fraction of IRF5 positive nuclei 1hr after CL75 stimulation (mean +SEM). (E) Fraction of p65 positive nuclei 1hr after CL75 stimulation. (F) Fraction of p65 positive nuclei 1hr after FSL-1 stimulation. The effect of inhibitors was tested by 1way ANOVA with Dunnett's Multiple Comparison Test against the "no inhibitor condition". (G, H) Effects of gene silencing of various targets in MDMs on the induction of IRF5 and p65 nuclear translocation by SA. Live SA Δ*lgt* ($3x10^7$/ml) including bacterial culture medium was added to the macrophages for 3 hrs. The fraction of positive nuclei from independent experiments is shown (mean +SEM, n=4). The

effect of targeted siRNAs was tested by 1way RM ANOVA with Dunnett's Multiple Comparison Test against Ctrl siRNA. *p <0.05, **p <0.01, ***p <0.001. Scalebar = 30 um.

Fig. 8. Model of TLR2- and TLR8- activation by SA and cross-regulation of the signaling pathways in human primary monocytes and MDMs. SA lipoproteins activate TLR2 leading to CR3 (CD11b/CD18) up-regulation on the monocyte surface and enhanced phagocytosis. Degradation of SA in the phagolysosome releases bacterial ssRNA which activates TLR8 signaling. Both TLR2 and TLR8 signal via the adaptor molecule MyD88 in TAK1 dependent and TAK1 independent pathways. The TAK1 independent pathway activates NF-kB p65 nuclear translocation in an IKKβ dependent fashion and is important for pro-inflammatory cytokine production. Both TLRs activate MAPKs by the TAK1 dependent pathway, but only TLR8 activate IRF5 nuclear translocation via a mechanism involving TAK1 and IKKβ. IRF5 nuclear accumulation via TLR8 signaling is a specific requirement for IFNβ and IL12 induction by SA, and also contributes to TNF production, while IL1 and IL18 are IRF5 independent. TLR2-activation inhibits TLR8-IRF5-signaling, probably at the level of TAK1/IKKβ or upstream.

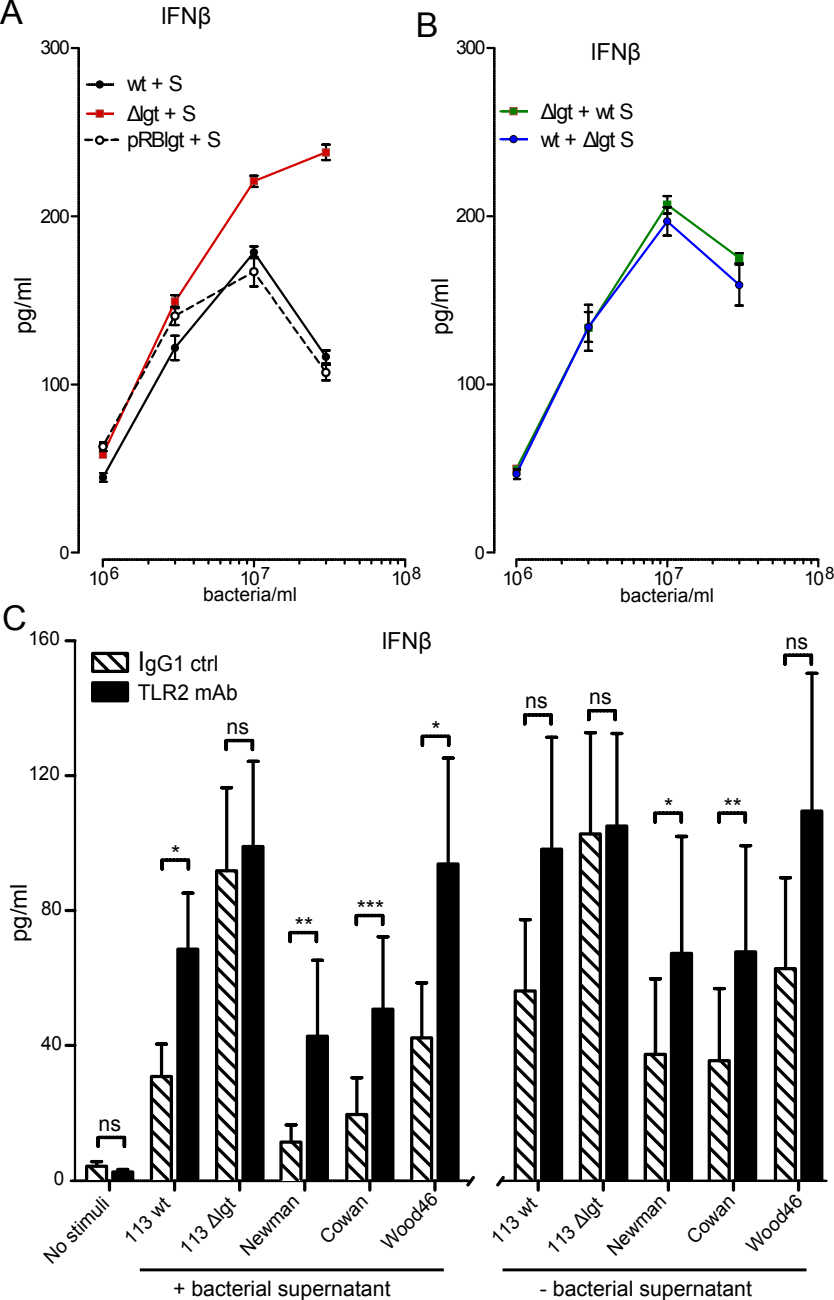
A
IFNβ
300
200
100
0
pg/ml
wt + S
Δlgt + S
pRBlgt + S
10^6
10^7
10^8
bacteria/ml
B
IFNβ
Δlgt + wt S
wt + Δlgt S
C
IgG1 ctrl
TLR2 mAb
IFNβ
160
120
80
40
0
ns
*
**
***
No stimuli
113 wt
113 Δlgt
Newman
Cowan
Wood46
+ bacterial supernatant
- bacterial supernatant

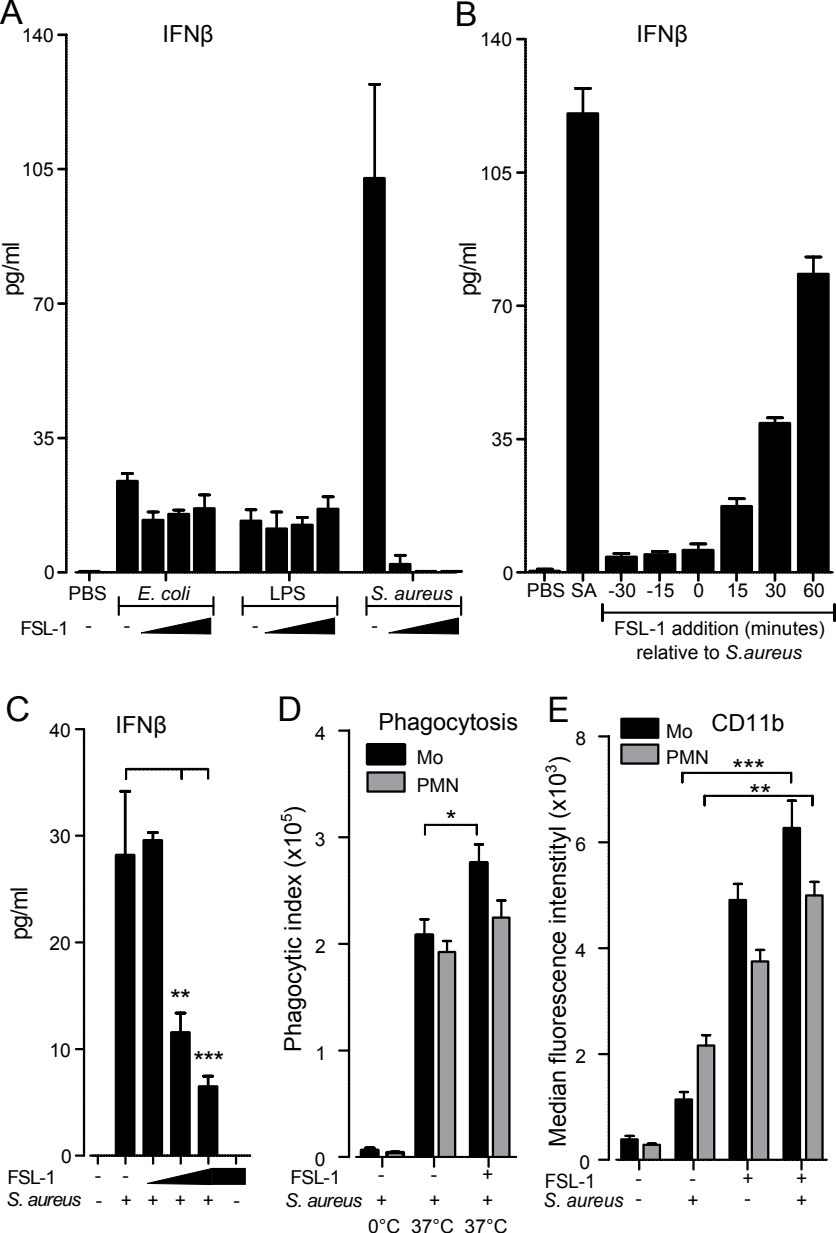
A
IFNβ
140
105
70
35
0
pg/ml
PBS
E. coli
LPS
S. aureus
FSL-1
B
IFNβ
140
105
70
35
0
pg/ml
PBS SA -30 -15 0 15 30 60
FSL-1 addition (minutes)
relative to S.aureus
C
IFNβ
40
30
20
10
0
pg/ml
**
***
FSL-1
S. aureus
D
Phagocytosis
Mo
PMN
*
Phagocytic index (x10^5)
4
3
2
1
0
FSL-1
S. aureus
0°C 37°C 37°C
E
Mo
PMN
CD11b
***
**
Median fluorescence intenstityl (x10^3)
8
6
4
2
0
FSL-1
S. aureus

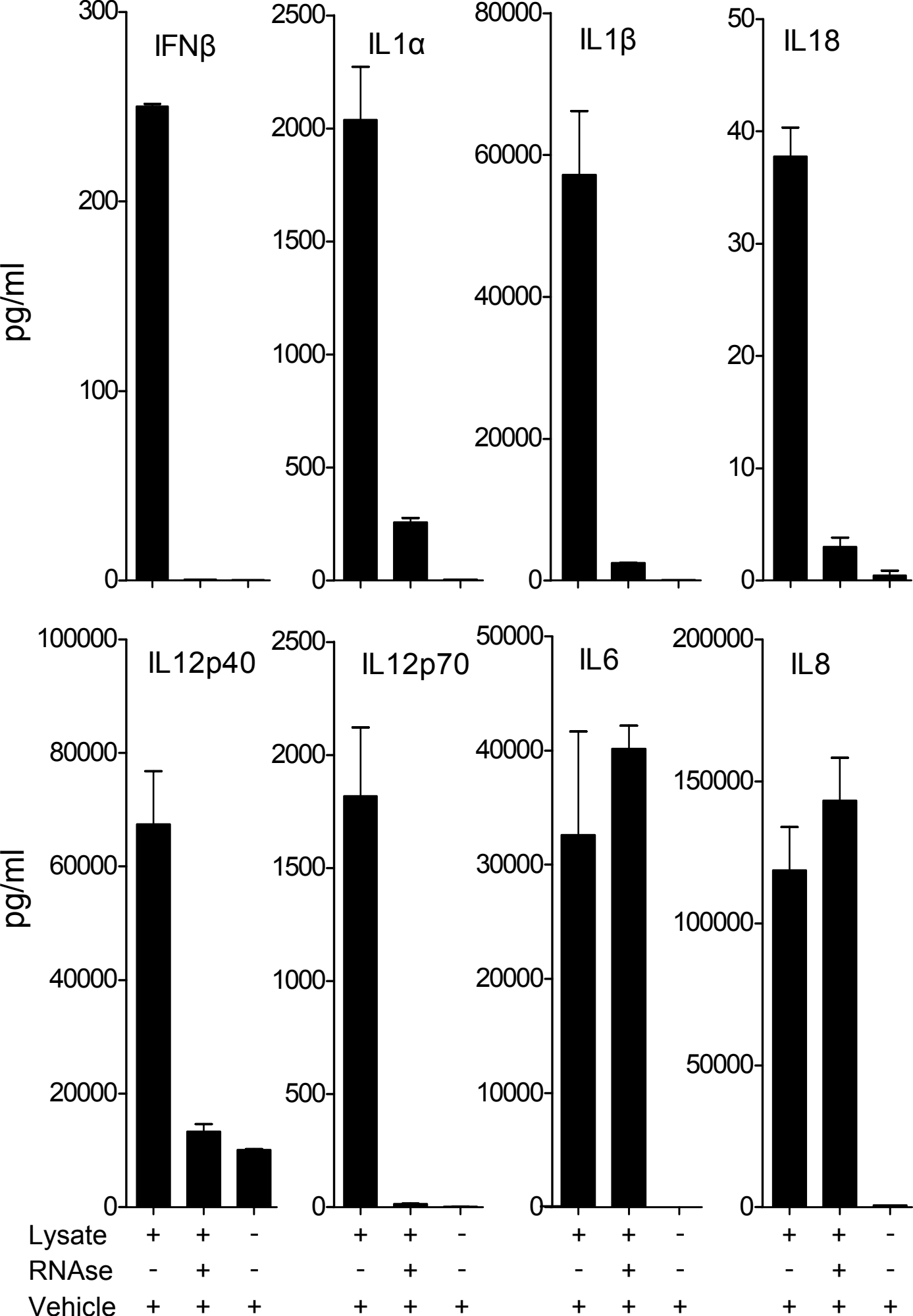
IFNβ
IL1α
IL1β
IL18
IL12p40
IL12p70
IL6
IL8
pg/ml
pg/ml
300
200
100
0
2500
2000
1500
1000
500
0
80000
60000
40000
20000
0
50
40
30
20
10
0
100000
80000
60000
40000
20000
0
2500
2000
1500
1000
500
0
50000
40000
30000
20000
10000
0
200000
150000
100000
50000
0
Lysate + + - + + - + + - + + -
RNAse - + - - + - - + - - + -
Vehicle + + + + + + + + + + + +

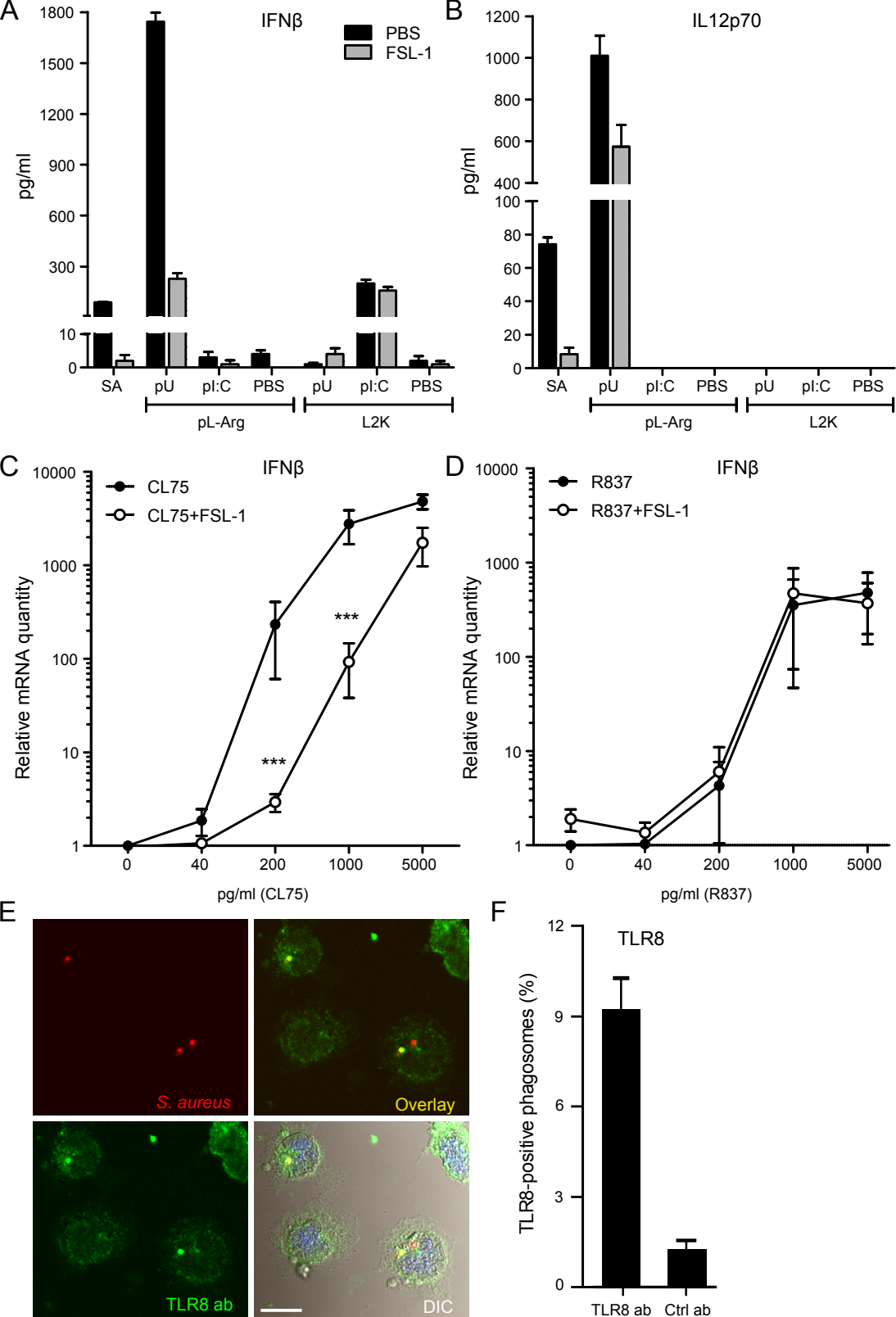
A
IFNβ
PBS
FSL-1
pg/ml
1800
1500
1200
900
600
300
10
0
SA
pU
pI:C
PBS
pU
pI:C
PBS
pL-Arg
L2K
B
IL12p70
pg/ml
1200
1000
800
600
400
100
80
60
40
20
0
SA
pU
pI:C
PBS
pU
pI:C
PBS
pL-Arg
L2K
C
IFNβ
CL75
CL75+FSL-1
Relative mRNA quantity
10000
1000
100
10
1
***
***
0
40
200
1000
5000
pg/ml (CL75)
D
IFNβ
R837
R837+FSL-1
Relative mRNA quantity
10000
1000
100
10
1
0
40
200
1000
5000
pg/ml (R837)
E
S. aureus
Overlay
TLR8 ab
DIC
F
TLR8
TLR8-positive phagosomes (%)
12
9
6
3
0
TLR8 ab
Ctrl ab

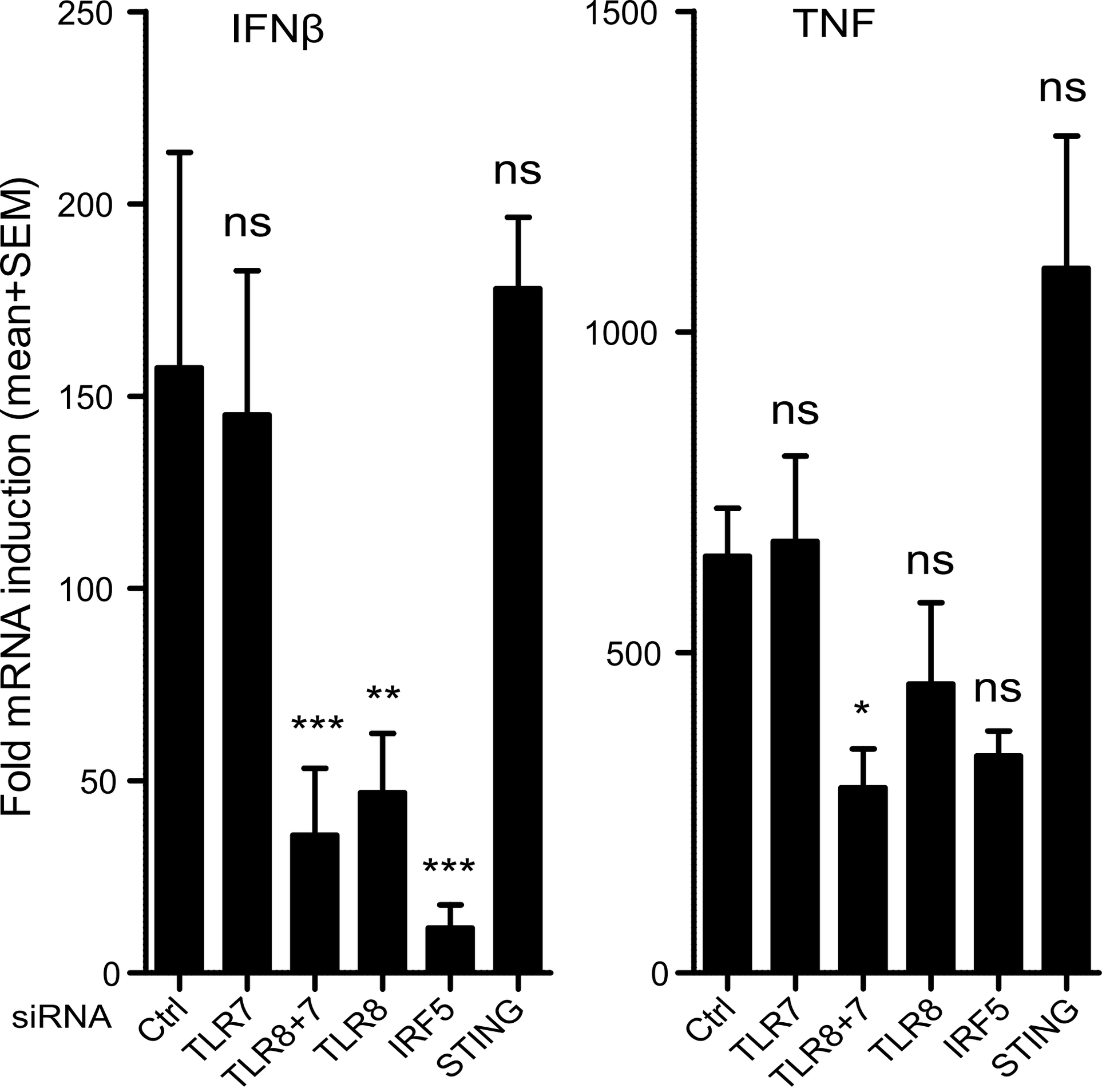
IFNβ
TNF
Fold mRNA induction (mean+SEM)
250
200
150
100
50
0
1500
1000
500
0
ns
ns
***
**
***
ns
ns
*
ns
ns
siRNA
Ctrl
TLR7
TLR8+7
TLR8
IRF5
STING

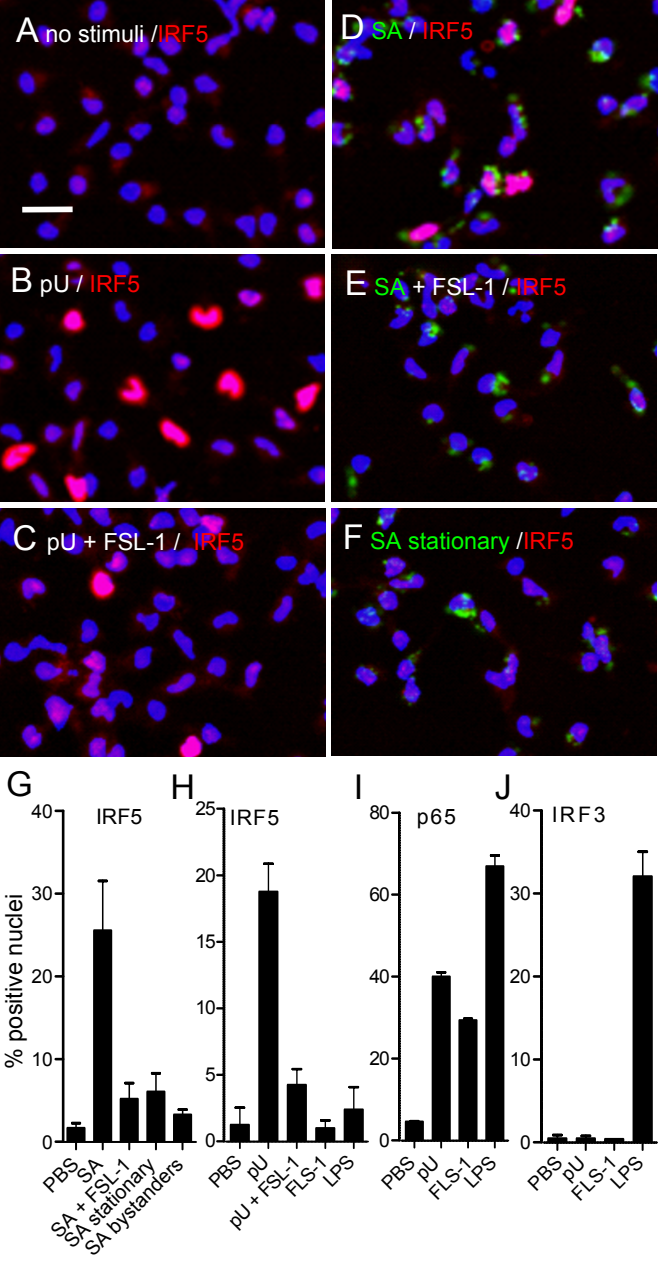
A no stimuli / IRF5
D SA / IRF5
B pU / IRF5
E SA + FSL-1 / IRF5
C pU + FSL-1 / IRF5
F SA stationary / IRF5
G
IRF5
% positive nuclei
PBS
SA
SA + FSL-1
SA stationary
SA bystanders
H
IRF5
PBS
pU
pU + FSL-1
FLS-1
LPS
I
p65
PBS
pU
FLS-1
LPS
J
IRF3
PBS
pU
FLS-1
LPS

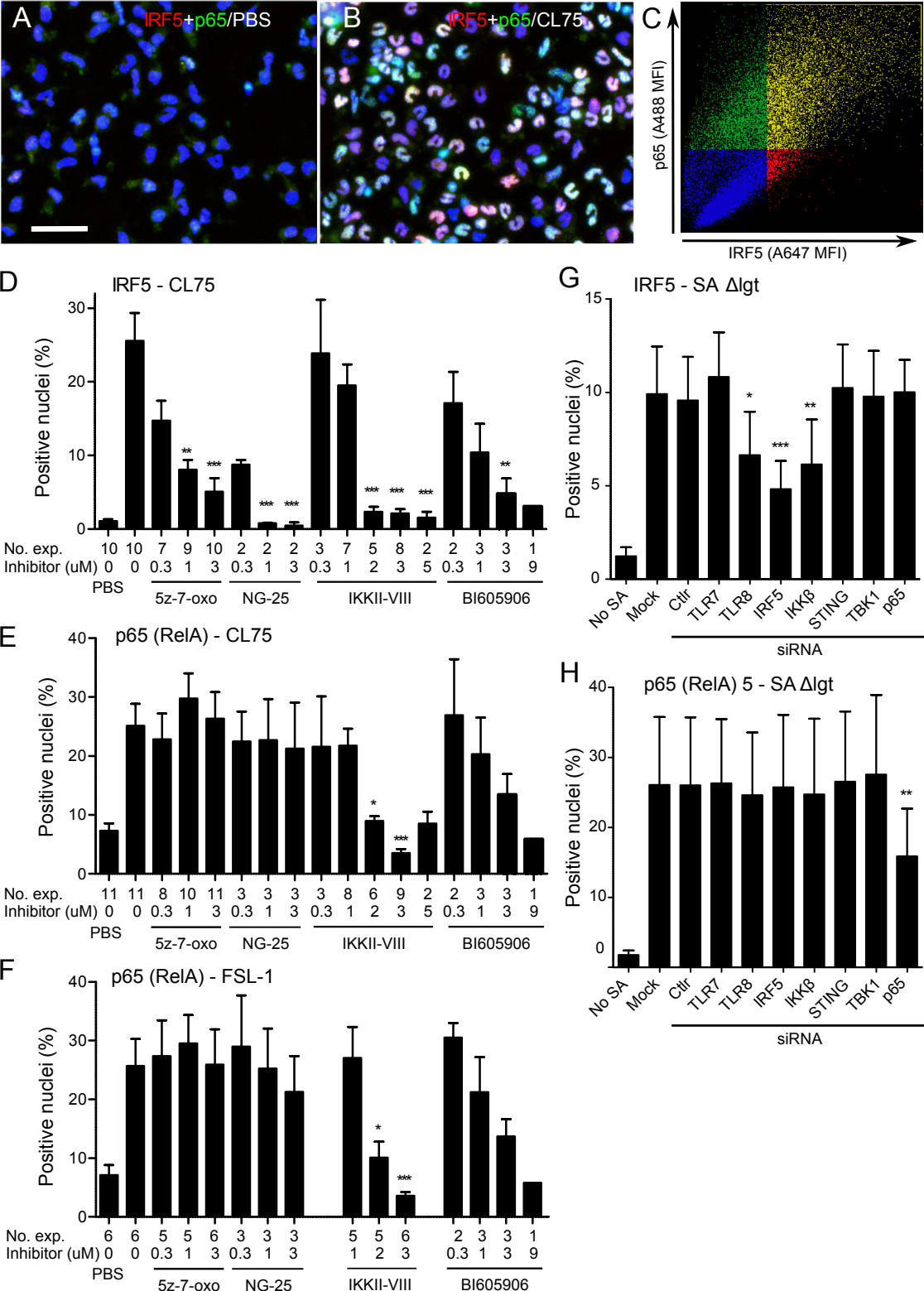
A
IRF5+p65/PBS
B
IRF5+p65/CL75
C
p65 (A488 MFI)
IRF5 (A647 MFI)
D
IRF5 - CL75
Positive nuclei (%)
No. exp.
Inhibitor (uM)
PBS
5z-7-oxo
NG-25
IKKII-VIII
BI605906
E
p65 (RelA) - CL75
F
p65 (RelA) - FSL-1
G
IRF5 - SA Δlgt
No SA
Mock
Ctlr
TLR7
TLR8
IRF5
IKKβ
STING
TBK1
p65
siRNA
H
p65 (RelA) 5 - SA Δlgt

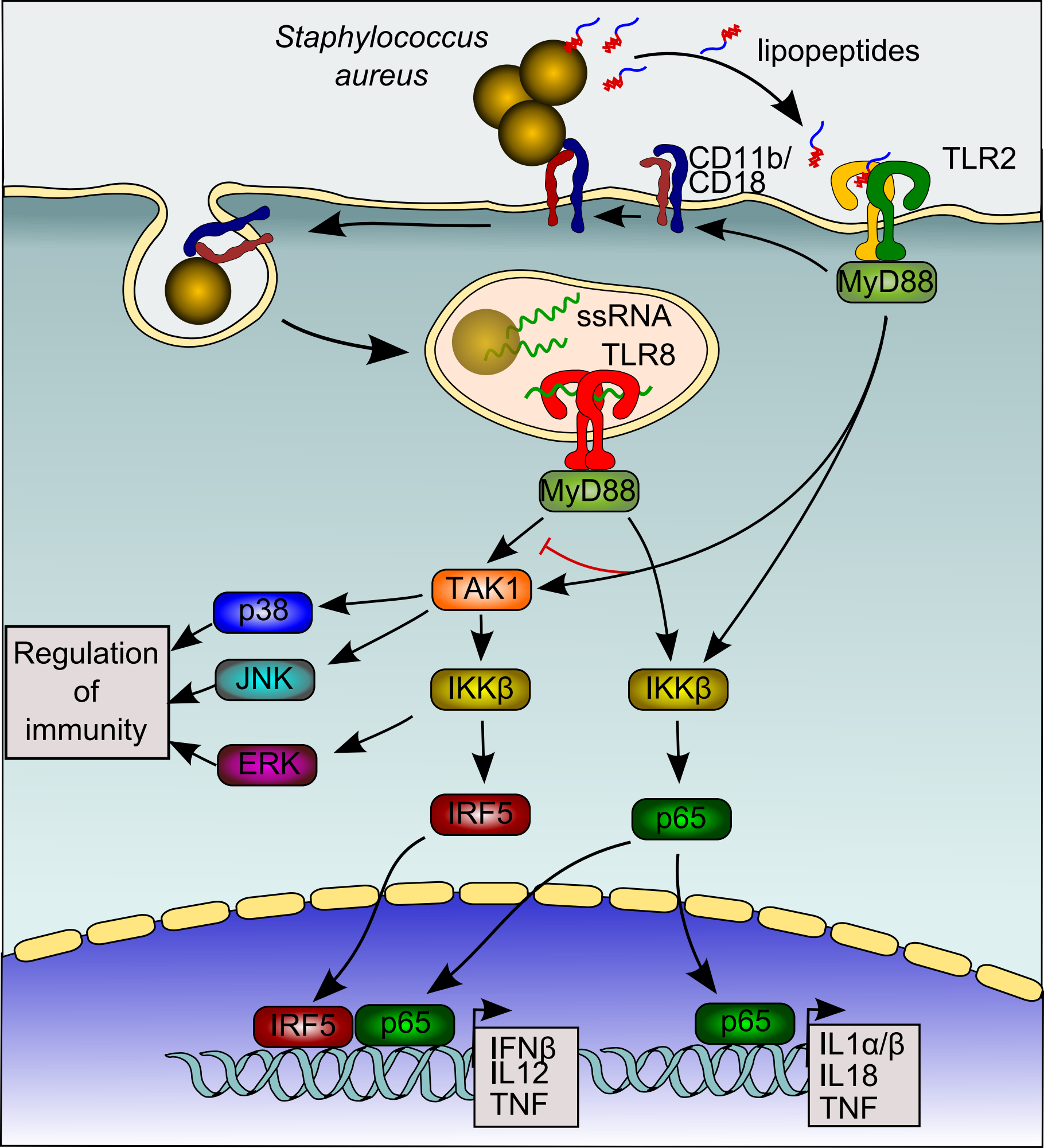
Staphylococcus aureus
lipopeptides
CD11b/ CD18
TLR2
MyD88
ssRNA
TLR8
MyD88
TAK1
p38
JNK
ERK
Regulation of immunity
IKKβ
IKKβ
IRF5
p65
IRF5
p65
IFNβ IL12 TNF
p65
IL1α/β IL18 TNF

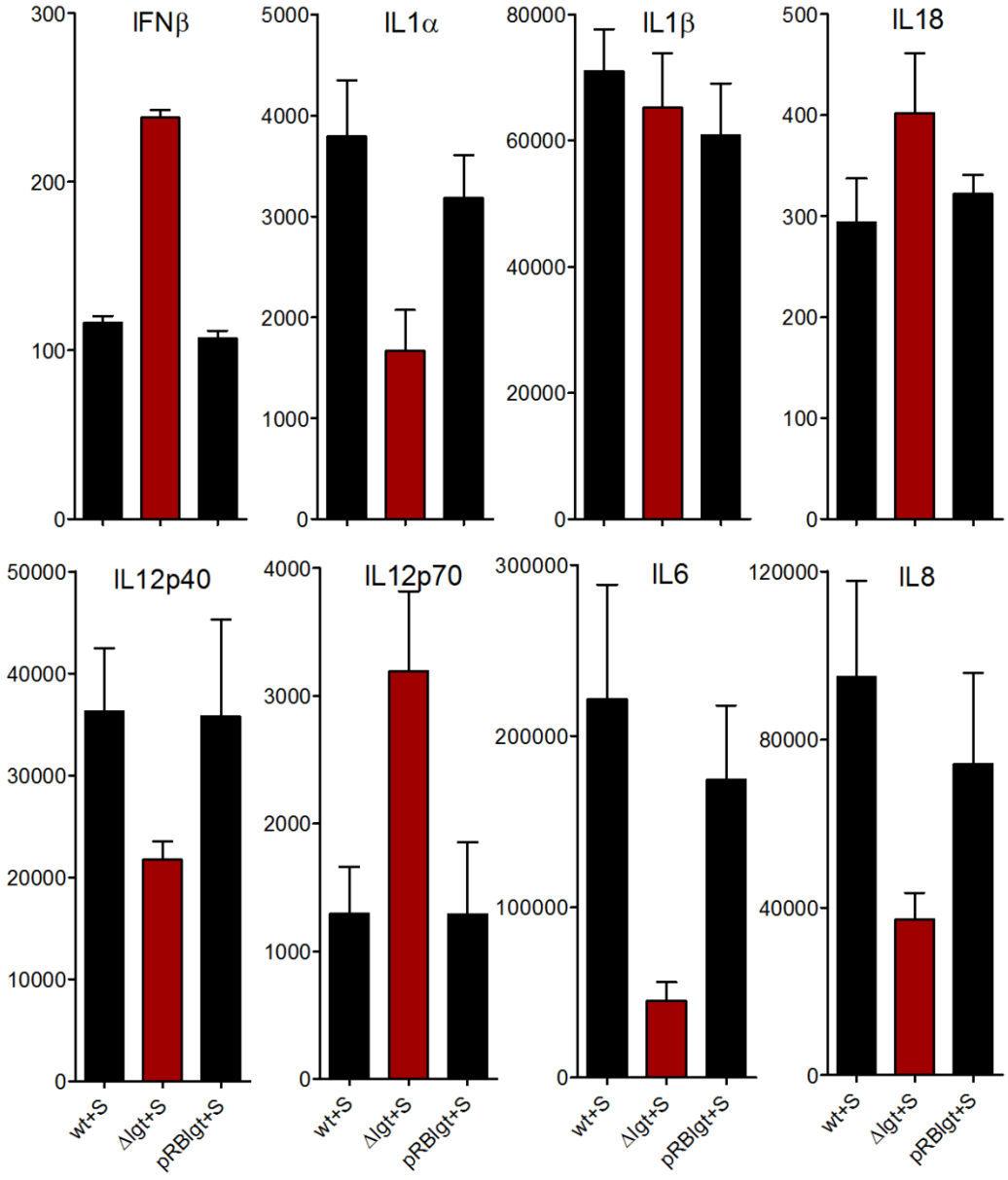

Fig. S1. TLR2 stimulatory lipopeptides of SA differentially regulate SA-induced cytokines in monocytes. Monocytes were infected with SA 113 wt-strain, its isogenic *lgt*-mutant (*Δlgt*), or the plasmid-reconstituted *Δlgt* strain (pRBlgt) including the bacterial culture supernatant 'S'. Extracellular bacteria were killed with gentamycin after 1hr and cell-culture supernatant was sampled 5hrs later. Monocyte supernatants in triplicates were analyzed for various cytokines with BioPlex (mean+SD of triplicates). One representative experiment out of two is shown.

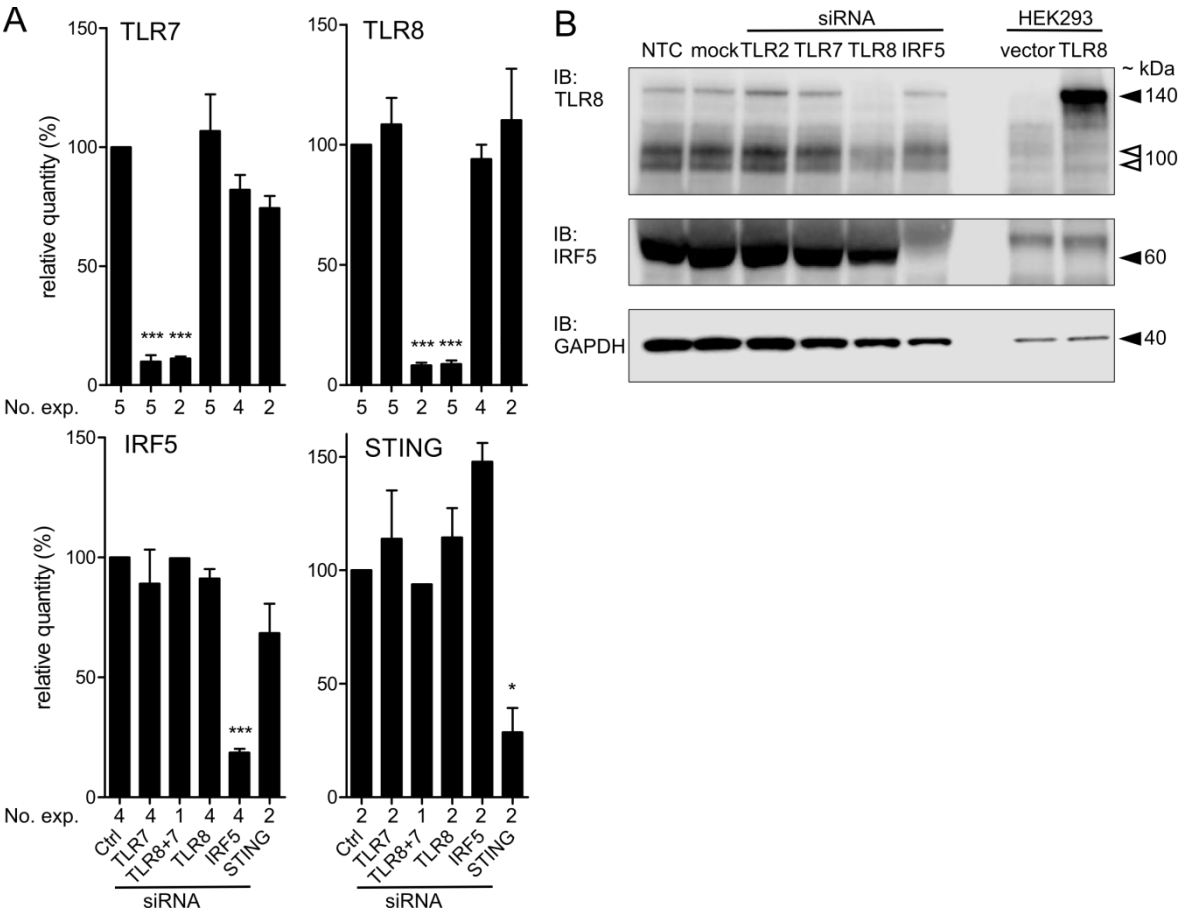

Fig. S2. Gene silencing of primary human macrophages. Monocyte derived macrophages were treated with siRNA by two times transient transfection (3+3 days). (A) Gene expression was determined with Q-PCR. Each experiment was conducted with triplicates and the expression levels were normalized to non-targeting Ctrl siRNA and merged (mean +SEM). 1way ANOVA; *P<0.05, **P<0.01, ***P<0.001. (B) Western blot analysis of TLR8 and IRF5 in siRNA treated macrophages and control lysate of HEK293 cells with or without transient expression of full length human TLR8. One representative out of two experiments is shown.

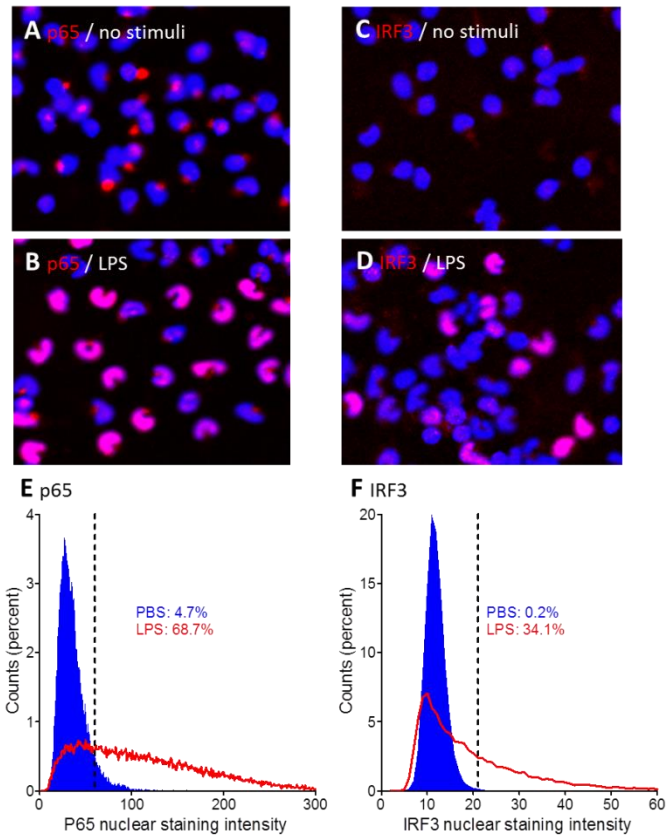

Fig. S3. Quantitative immunoflouresence analyses of nuclear p65 and IRF3 accumulation in monocytes by LPS-stimulation. Monocytes were left untreated (A, C) or stimulated with *E. coli* K12 LPS (100ng/ml) (B, D) for 1 hour. Immunostaining of transcription factors was done and fluorescent images were captured with the Scan^R high-content screening system (Olympus) with a 20 x objective. Nuclei were stained with Hoechst dye (blue). (A, B) Staining of total p65 (RelA, red). (C, D) Staining of total IRF3 (red). Quantification of the frequency of cells with positive nuclear staining of transcription factors was done by automated image acquisition and analysis using the Scan^R, and 100 frames/well (approx. 5000-15000 cells) were analyzed. (E) Frequency distributions and percent of p65 (RelA) positive nuclei. (F) Frequency distributions and percent of IRF3 positive nuclei. Threshold levels for scoring of positively stained nuclei were defined by visual inspection of images and are shown as vertical hatched lines. The frequency distributions (mean nuclear staining intensity) were calculated and plotted with GraphPad Prism.

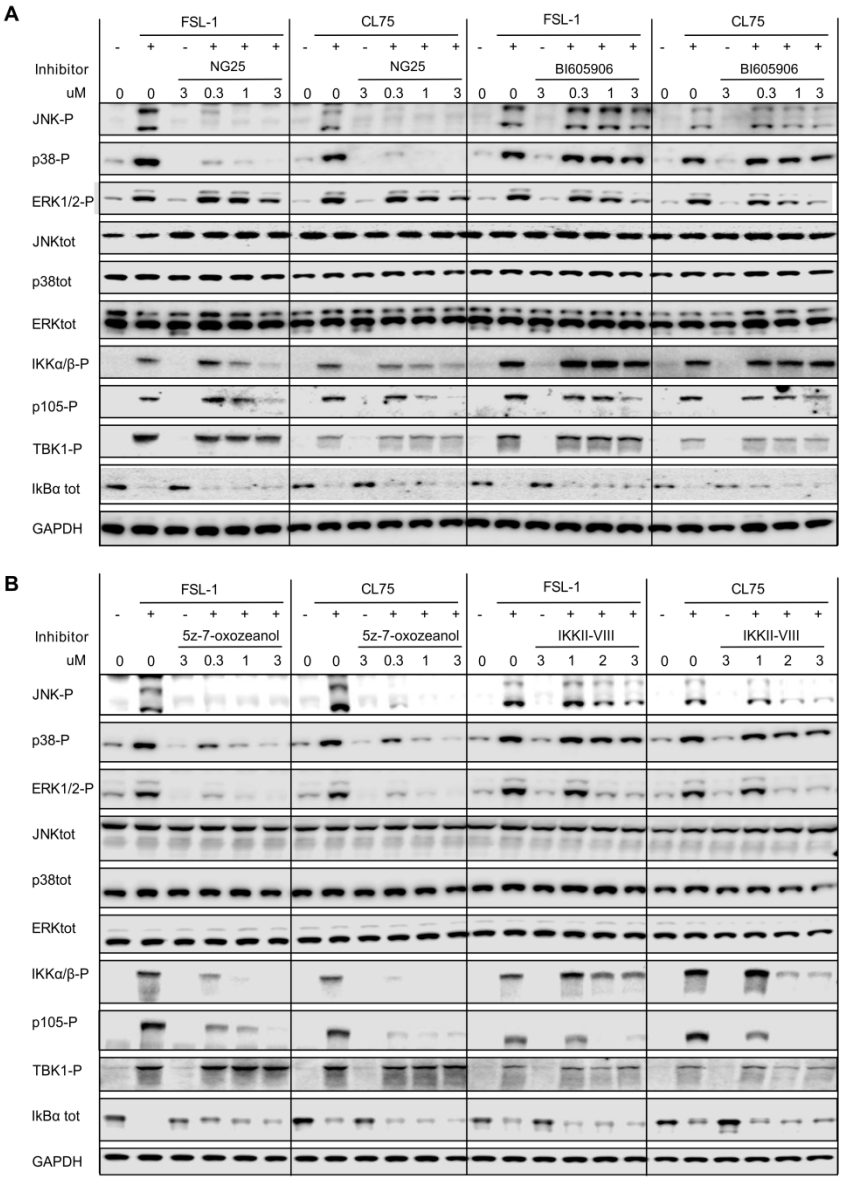

Fig. S4. Effects of TAK1 and IKKβ inhibitors on signaling intermediates after TLR8 and TLR2 activation. (A) Monocytes were pre-treated with NG-25 (TAK1 inhibitor) or BI605906 (IKKβ inhibitor) for 30 minutes and stimulated with CL75 or FSL-1 for 30 minutes. Cell lysates were analyzed by western blot for total and phosphorylated forms of JNK, p38 and ERK1/2 MAPKs, as well as phosphorylated forms of IKKα/β and p105 (NF-kB1, p50-precursor). (B) Same experiment with different inhibitors for TAK1 (5z-7-oxozeanol) and IKKβ (IKKII-VIII). One representative experiment out of three is shown**.**